LiDAR Remote Sensing Data Collection:

Upper & Lower Okanogan River, Methow River, Lake Roosevelt, Wenatchee River and John Day River Study Areas

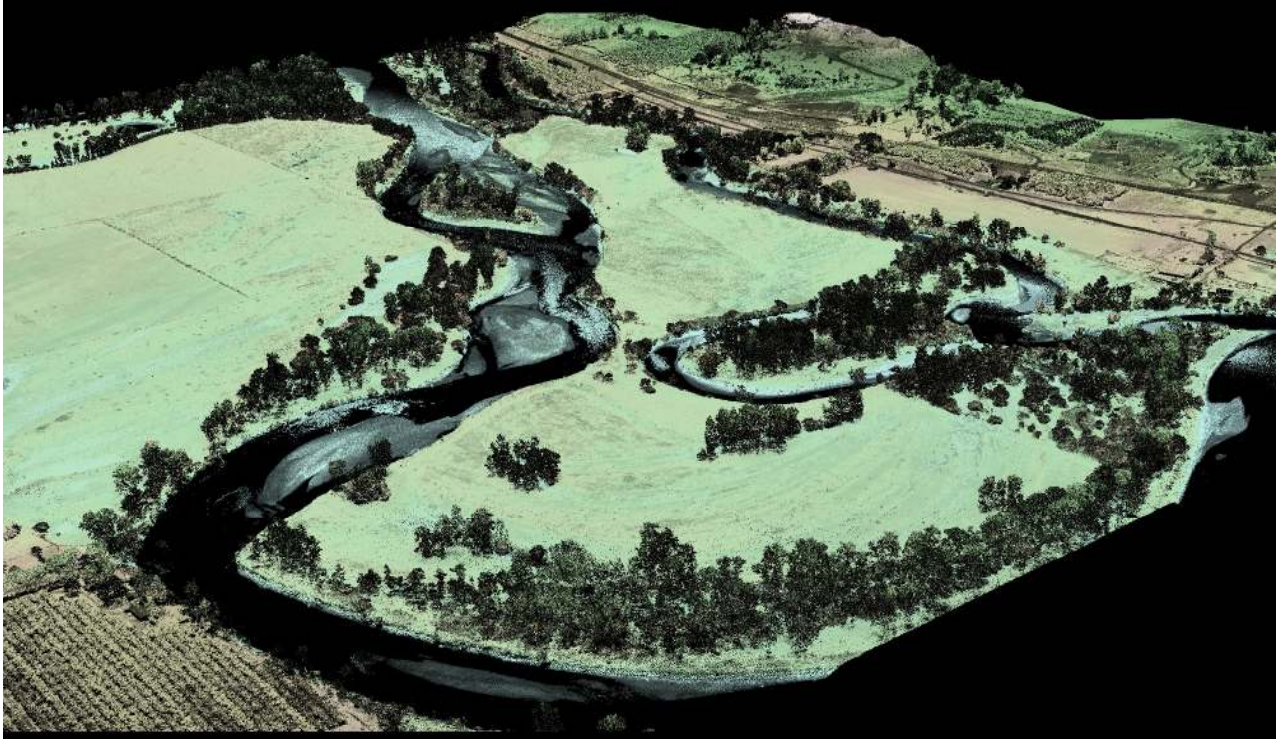

LiDAR-Derived Surface: Point Cloud of all Laser Returns, Shown by Intensity and Elevation, Lower Okanogan River Study Area

Submitted to:

Puget Sound LiDAR Consortium
Diana Martinez
Puget Sound Regional Council
1011 Western Avenue, Suite 500
Seattle, Washington 98104-1035

Submitted by:

Watershed Sciences
215 SE Ninth Avenue, Suite 106
Portland, Oregon 97214

April 18, 2007

LiDAR Remote Sensing Data Collection:
Upper & Lower Okanogan River, Methow River, Lake Roosevelt, Wenatchee River, John Day River Study Areas

TABLE OF CONTENTS

1. Introduction

Watershed Sciences, Inc. (WS) collected Light Detection and Ranging (LiDAR) data in eastern Washington, eastern Oregon, and southern Canada in October and November, 2006 for the Puget Sound LiDAR Consortium. The survey areas cover portions of the upper Okanogan River in Canada, the lower Okanogan River in Washington, the Methow River in Washington, Lake Roosevelt in Washington, the Wenatchee River in Washington, and the John Day River in Oregon. The map below (**Figure 1**) illustrates the extents and naming convention applied to each study area for the purposes of this data report.

Figure 1. Extents of Upper and Lower Okanogan River, Methow River, Lake Roosevelt, Wenatchee River and John Day River study areas.

The total delivered acreage for the study areas shown above is ~26,000 acres greater than the original amount, due to buffering of the original study areas and flight planning optimization.

Table 1. Acreage summary.

Study Area	Original Acres	Delivered Acres
Upper Okanogan (CN)	20,181	23,972
Lower Okanogan (WA)	12,201	15,512
Methow (WA)	34,125	45,162
Lake Roosevelt (WA)	92,001	99,072
John Day (OR)	7,847	9,148
Wenatchee (WA)	35,184	43,787
TOTALS:	**201,539**	**236,752**

Laser points were collected over the study areas using a LiDAR laser system set to acquire points with full overlap (i.e., ≥50% side-lap) to ensure complete coverage and minimize laser shadows created by buildings and tree canopies. A real-time kinematic (RTK) survey was conducted throughout the study area for quality assurance purposes. The accuracy of the LiDAR data is described as standard deviations of divergence (sigma ~ σ) from RTK ground survey points and root mean square error (RMSE) which considers bias (upward or downward).

For all study areas, deliverables include point data in ASCII and *.las v.1.1 format, 0.5-meter resolution laser intensity images, 0.5-meter contours, 1-meter resolution bare ground model ESRI GRIDs, and 1-meter resolution Highest Hit vegetation model ESRI GRIDs. Data are delivered in Universal Transverse Mercator (UTM) Zone 10/11, in the NAD83/NAVD88 datum (Geoid 03). Please see Table 2 below for details.

2. Acquisition

2.1 Airborne Survey – Instrumentation and Methods

The LiDAR surveys utilized two different laser systems—the Leica ALS50 Phase II and the Optech 3100. Flight parameters were different for each system, resulting in different native pulse densities (the number of pulses emitted by the LiDAR system from the aircraft).

Some types of surfaces (i.e., dense vegetation or water) may return fewer pulses than the laser originally emitted. Therefore, the delivered density can be less than the native density and lightly variable according to distributions of terrain, land cover and water bodies. All study areas were surveyed with opposing flight line side-lap of ≥50% (≥100% overlap) to reduce laser shadowing and increase surface laser painting. Both laser systems allow up to four range measurements per pulse, and all discernable laser returns were processed for the output dataset.

Table 2 below summarizes the instrumentation, specifications, and datum/projection for each study area.

Table 2. Instrumentation and specifications.

Study Area	LiDAR System	Collection Dates	Pulse Rate	Point Density	Scan Angle	Datum / Projection
Upper Okanogan (CN)	Optech 3100	11/01/06 and 11/05/06 *(Julian Day 305, 309)*	71 kHz	≥4 pts/m²	±14° from nadir	UTM Zone 11 NAD83/NAVD88 datum (Geoid 03)
Lower Okanogan (WA)	Leica ALS50 Phase II	11/05/06 *(Julian Day 309)*	115 kHz	≥8 pts/m²	±13° from nadir	UTM Zone 11 NAD83/NAVD88 datum (Geoid 03)
Methow (WA)	Leica ALS50 Phase II	11/08/06-11/09/06 *(Julian Day 312-313)*	115 kHz	≥8 pts/m²	±13° from nadir	UTM Zone 10 NAD83/NAVD88 datum (Geoid 03)
Lake Roosevelt (WA)	Leica ALS50 Phase II	10/16/06-10/20/06 & 10/29/06-11/01/06 *(Julian Days 289-293 & 302-305)*	115 kHz	≥8 pts/m²	±13° from nadir	UTM Zone 11 NAD83/NAVD88 datum (Geoid 03)
John Day (OR)	Leica ALS50 Phase II	10/05/06-10/07/06 *(Julian Day 278-280)*	115 kHz	≥8 pts/m²	±13° from nadir	UTM Zone 11 NAD83/NAVD88 datum (Geoid 03)
Wenatchee, (WA)	Optech 3100	10/12/06-10/13/06 (Julian Day 285-286)	71 kHz	≥4 pts/m²	±14° from nadir	UTM Zone 10 NAD83/NAVD88 datum (Geoid 03)
Wenatchee, (WA)	Leica ALS50 Phase II	10/25/06-10/28/06 (Julian Day 298-301)	115 kHz	≥8 pts/m²	±13° from nadir	UTM Zone 10 NAD83/NAVD88 datum (Geoid 03)

To solve for laser point position, it is vital to have an accurate description of aircraft position and attitude. Aircraft position is described as x, y and z and measured twice per second (2 Hz) by an onboard differential GPS unit. Aircraft attitude is measured 200 times per second (200 Hz) as pitch, roll and yaw (heading) from an onboard inertial measurement unit (IMU).

2.2 Ground Survey – Instrumentation and Methods

During the LiDAR surveys of all study areas, multiple static (1 Hz recording frequency) ground surveys were conducted over monuments with known coordinates. Coordinates are provided in **Table 3** and shown in **Figure 2**. After the airborne survey, the static GPS data are processed using triangulation with CORS stations and checked against the Online Positioning User Service (OPUS[1]) to quantify daily variance. Multiple sessions are processed over the same monument to confirm antenna height measurements and reported position accuracy.

Table 3. Base Station Surveyed Coordinates, (NAD83/NAVD88, OPUS corrected) used for kinematic post-processing of the aircraft GPS data for all study areas.

		Datum NAD83(CORS96)		GRS80
Study Area	Base Station ID	Latitude (North)	Longitude (West)	Ellipsoid Height (m)
John Day	JD1	44°57'38.89072"N	118°55'54.07447"W	1160.753
John Day	JD2	44°57'38.93670"N	118°55'52.46293"W	1162.685
John Day	MF1	44°37'14.43008"N	118°34'10.27072"W	1193.675
John Day	MF2	44°36'44.91972"N	118°32'59.31593"W	1201.925
Wenatchee	WSDOT	47°33'29.02659"N	120°35'26.23803"W	308.433
Wenatchee	AE1857	47°46'04.73508"N	120°39'53.83277"W	548.611
Wenatchee	PL1	47°46'04.53598"N	120°39'53.74850"W	548.8
Lake Roosevelt	RS1	48°41'34.56034"N	118°04'19.57855"W	465.202
Lake Roosevelt	RS2	48°50'18.29820"N	117°56'28.75727"W	607.539
Lower Okanogan	LO1	48°50'05.22025"N	119°25'27.34273"W	271.408
Lower Okanogan	LO2	48°50'05.30873"N	119°25'27.51225"W	271.703
Lower Okanogan	SAL2	48°27'37.49710"N	119°31'02.09418"W	376.168
Methow	X378	48°25'30.42258"N	120°08'43.50943"W	499.038
Methow	Win1	48°36'00.50491"N	120°10'01.35337"W	631.236
		Datum NAD83(CSRS2002)		CGVD1928
Study Area	Base Station ID	Latitude (North)	Longitude (West)	Ellipsoid Height (m)
Upper Okanogan	PEN1	49°14'20.38706"N	119°31'30.00977"W	301.014
Upper Okanogan	PEN2	49°18'12.45051"N	119°32'03.43372"W	314.073
Upper Okanogan	PEN3	49°27'29.97893"N	119°36'25.46381"W	323.825

Multiple Thales Z-max DGPS units are used for the ground real-time kinematic (RTK) portion of the survey. To collect accurate ground surveyed points, a GPS base unit is set up over

[1] Online Positioning User Service (OPUS) is run by the National Geodetic Survey to process corrected monument positions.

monuments to broadcast a kinematic correction to a roving GPS unit. The ground crew uses a roving unit to receive radio-relayed kinematic corrected positions from the base unit. This method is referred to as real-time kinematic (RTK) surveying and allows precise location measurement ($\sigma \leq 1.5$ cm ~ 0.6 in). **Figures 3-4** below show examples of RTK point locations in the Lower Okanogan study area.

Figure 2. Base station locations in all study areas.

Figure 3. Locations of Base Stations and RTK Survey Point Collection along the Lower Okanogan River in the **Lower Okanogan study area**.

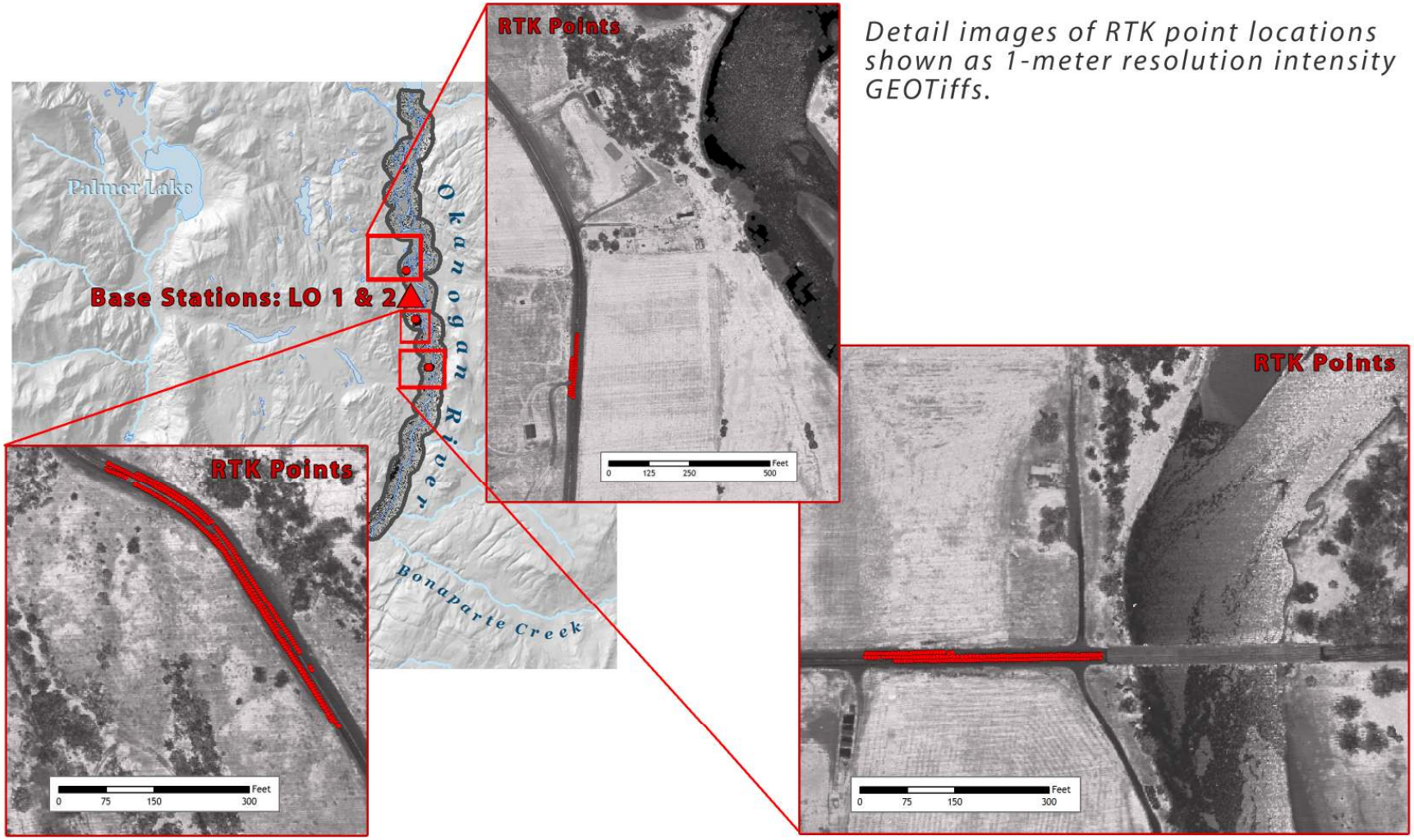

Figure 4. Locations of Base Stations and RTK Survey Point Collection along Salmon Creek in the **Lower Okanogan study area**.

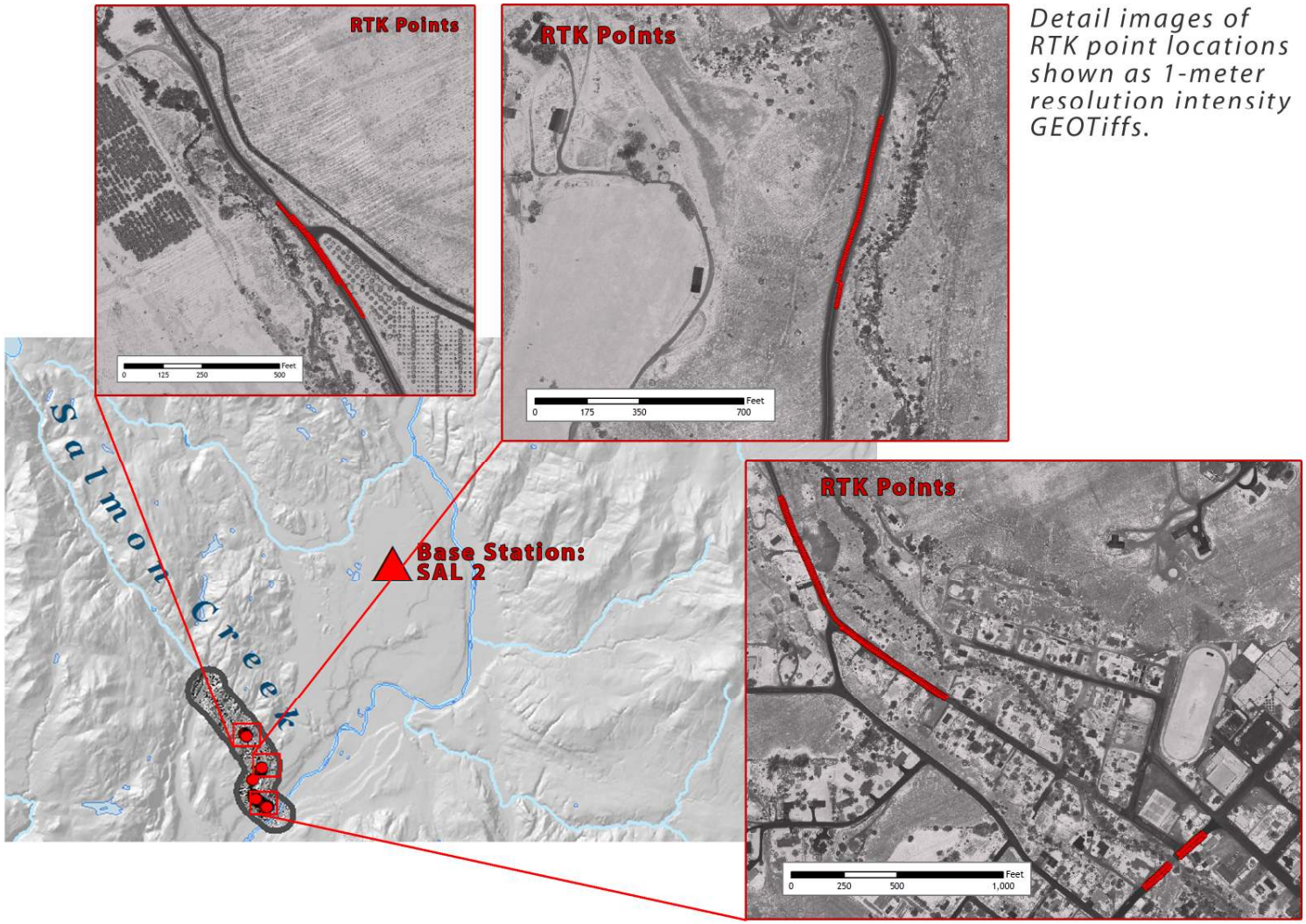

3. LiDAR Data Processing

3.1 Applications and Work Flow Overview

1. Resolve kinematic corrections for aircraft position data using kinematic aircraft GPS and static ground GPS data.
   Software: Waypoint GPS v.7.60, REALM
2. Develop a smoothed best estimate of trajectory (SBET) file that blends the post-processed aircraft position with attitude data. Sensor head position and attitude are calculated throughout the survey. The SBET data are used extensively for laser point processing.
   Software: IPAS v.1.0, POSPAC
3. Calculate laser point position by associating the SBET position to each laser point return time, scan angle, intensity, etc. Creates raw laser point cloud data for the entire survey in *.las (ASPRS v1.1) format.
   Software: ALS Post Processing Software, REALM
4. Import raw laser points into manageable blocks (less than 500 MB) to perform manual relative accuracy calibration and filter for pits/birds. Ground points are then classified for individual flight lines (to be used for relative accuracy testing and calibration).
   Software: TerraScan v.6.009
5. Using ground classified points per each flight line, the relative accuracy is tested. Automated line-to-line calibrations are then performed for system attitude parameters (pitch, roll, heading), mirror flex (scale) and GPS/IMU drift. Calibrations are performed on ground classified points from paired flight lines. Every flight line is used for relative accuracy calibration.
   Software: TerraMatch v.6.009
6. Position and attitude data are imported. Resulting data are classified as ground and non-ground points. Statistical absolute accuracy is assessed via direct comparisons of ground classified points to ground RTK survey data. Data are then converted to orthometric elevations (NAVD88) by applying a Geoid03 correction. Ground models are created as a triangulated surface and exported as ArcInfo ASCII grids. Highest Hit model surfaces are developed from all points and exported as ArcInfo ASCII grids. Intensity images (GeoTIFF format) are created with averages of the laser footprint. Contours are developed from ground-classified points in *.dxf format and converted to shapefile format.
   Software: TerraScan v.6.009, ArcMap v9.1
7. The bin-delineated LAS files (ASPRS v1.0) are converted to ASCII format, preserving all LAS fields.
   Software: Custom

3.2 Aircraft Kinematic GPS and IMU Data

LiDAR survey datasets are referenced to 1-Hz static ground GPS data collected over pre-surveyed monuments with known coordinates. While surveying, the aircraft collects 2 Hz kinematic GPS data. The onboard inertial measurement unit (IMU) collects 200 Hz aircraft attitude data. Waypoint GPS v.7.60 and REALM are used to process the kinematic corrections for the aircraft. The static and kinematic GPS data are then post-processed after the survey to obtain an accurate GPS solution and aircraft positions. IPAS v.1.0 and POSPAC are used to develop a trajectory file that includes corrected aircraft position and attitude information. The trajectory data for the entire flight survey session are incorporated into a final smoothed best estimate trajectory (SBET) file that contains accurate and continuous aircraft positions and attitudes.

3.3 Laser Point Processing

Laser point coordinates are computed using the IPAS and POSPAC software suites based on independent data from the LiDAR system (pulse time, scan angle), and aircraft trajectory data (SBET). Laser point returns (first through fourth) are assigned an associated (x, y, z) coordinate along with unique intensity values (0-255). The data are output into large LAS v. 1.1 files; each point maintains the corresponding scan angle, return number (echo), intensity, and x, y, z (easting, northing, and elevation) information.

These initial laser point files are too large to process (i.e. > 40 GB). To facilitate laser point processing, bins (polygons) are created to divide the dataset into manageable sizes (< 500 MB). The bins are approximately 1 km^2 each, as shown in **Figure 5** below.

Figure 5: Single bin example, 1-meter resolution bare earth model, Upper Okanogan River study area.

Flightlines and LiDAR data are then reviewed to ensure complete coverage of the study area and positional accuracy of the laser points.

Once the laser point data are imported into bins in TerraScan, a manual calibration is performed to assess the system offsets for pitch, roll, heading and mirror scale. Using a

geometric relationship developed by Watershed Sciences, each of these offsets is resolved and corrected if necessary.

The LiDAR points are then filtered for noise, pits and birds by screening for absolute elevation limits, isolated points and height above ground. Each bin is then inspected for pits and birds manually; spurious points are removed. For a bin containing approximately 7.5-9.0 million points, an average of 50-100 points are typically found to be artificially low or high. These spurious non-terrestrial laser points must be removed from the dataset. Common sources of non-terrestrial returns are clouds, birds, vapor, and haze.

Figure 6. Example of points removed from 0.9375-minute quads 48118-e1-nw-BB and 48118-e1-nw-BA in the **Lake Roosevelt study area.**

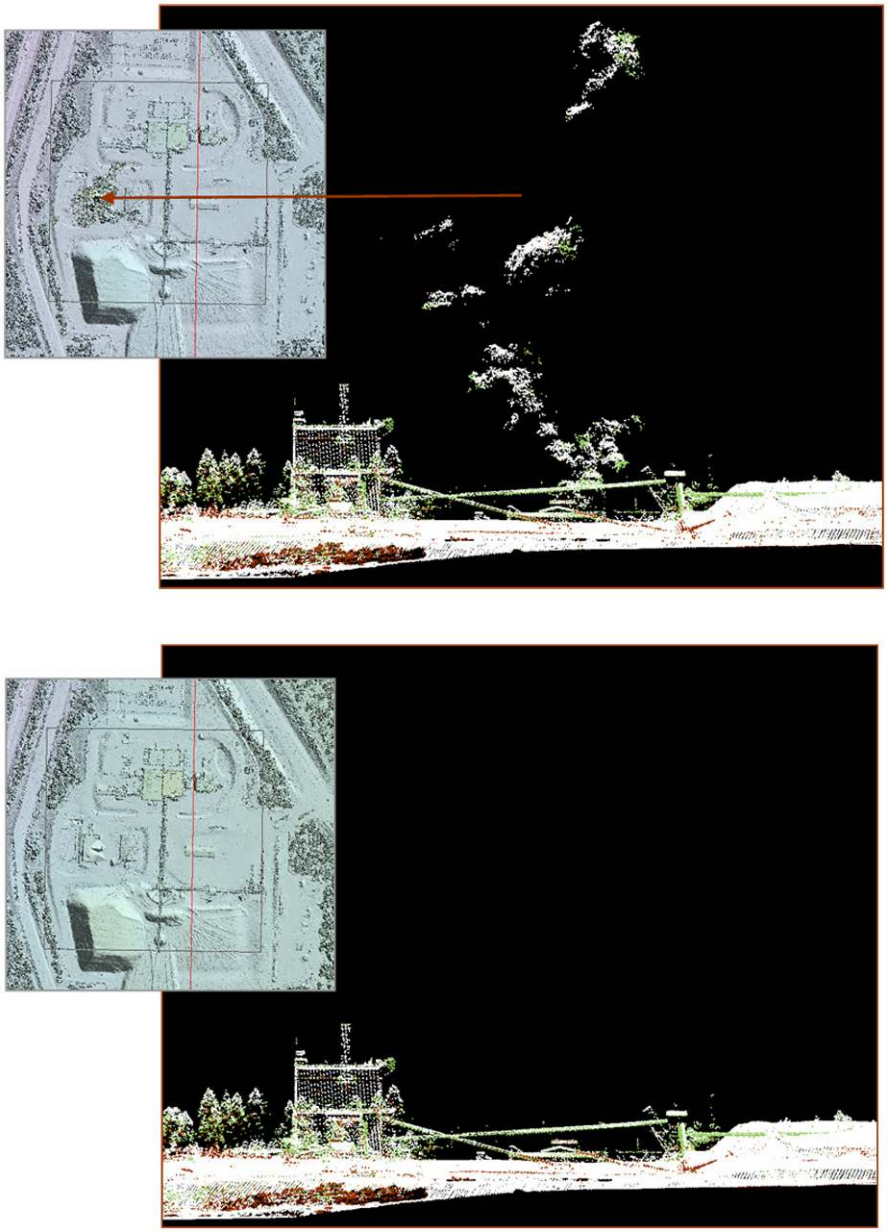

The internal calibration is refined using TerraMatch. Points from overlapping lines are tested for internal consistency and final adjustments are made for system misalignments (i.e., pitch, roll, heading offsets and mirror scale). Automated sensor attitude and scale corrections yield 3-5 cm improvements in the relative accuracy. Once the system misalignments are corrected, vertical GPS drift is then resolved and removed per flight line, yielding a slight improvement

(<1 cm) in relative accuracy. At this point in the workflow, data have passed a robust calibration designed to reduce inconsistencies from multiple sources (i.e. sensor attitude offsets, mirror scale, GPS drift) using a procedure that is comprehensive (i.e. uses all of the overlapping survey data). Relative accuracy screening is complete.

The TerraScan software suite is designed specifically for classifying near-ground points (Soininen, 2004). The processing sequence begins by 'removing' all points that are not 'near' the earth based on geometric constraints used to evaluate multi-return points. The resulting bare earth (ground) model is visually inspected and additional ground point modeling is performed in site-specific areas (over a 50-meter radius) to improve ground detail. This is only done in areas with known ground modeling deficiencies, such as: bedrock outcrops, cliffs, deeply incised stream banks, and dense vegetation. In some cases, ground point classification includes known vegetation (i.e., understory, low/dense shrubs, etc.) and these points are reclassified as non-grounds. Ground surface rasters and contour vector data are developed from triangulated irregular networks (TINs) of ground points.

4. LiDAR Accuracy

4.1 Laser Point Accuracy

Laser point absolute accuracy is largely a function of internal consistency (measured as relative accuracy) and laser noise:

- **Laser Noise**: For any given target, laser noise is the breadth of the data cloud per laser return (i.e., last, first, etc.). Lower intensity surfaces (roads, rooftops, still/calm water) experience higher laser noise. The laser noise range for these missions is approximately 0.02 meters.

- **Relative Accuracy**: Internal consistency refers to the ability to place a laser point in the same location over multiple flight lines, GPS conditions, and aircraft attitudes.

- **Absolute Accuracy**: RTK GPS measurements were taken throughout all study areas and are compared to LiDAR point data in each study area. The root mean square error (RMSE) is reported for each study area, along with 1- and 2-sigma absolute deviation values.

Table 4. LiDAR accuracy is a combination of several sources of error. These sources of error are cumulative. Some error sources that are biased and act in a patterned displacement can be resolved in post processing.

Type of Error	Source	Post Processing Solution	Effect
GPS (Static/Kinematic)	Long Base Lines	None	
	Poor Satellite Constellation	None	
	Poor Antenna Visibility	Reduce Visibility Mask	Slight
Relative Accuracy	Poor System Calibration	Recalibrate IMU and sensor offsets/settings	Large
	Inaccurate System	None	
Laser Noise	Poor Laser Timing	None	
	Poor Laser Reception	None	
	Poor Laser Power	None	
	Irregular Laser Shape	None	

4.1.1 Relative Accuracy

Relative accuracy refers to the internal consistency of the data set and is measured as the divergence between points from different flight lines within an overlapping area. Divergence is most apparent when flight lines are opposing. When the LiDAR system is well calibrated the line to line divergence is low (<10 cm). Internal consistency is affected by system attitude offsets (pitch, roll and heading), mirror flex (scale), and GPS/IMU drift.

Operational measures taken to improve relative accuracy:

1. Low Flight Altitude: Terrain following was targeted at a flight altitude of 800-1000 meters above ground level (AGL). Laser horizontal errors are a function of flight altitude above ground (i.e., ~ $1/3000^{th}$ AGL flight altitude). Lower flight altitudes decrease laser noise on surfaces with even the slightest relief.
2. Focus Laser Power at narrow beam footprint: A laser return must be received by the system above a power threshold to accurately record a measurement. The strength of the laser return is a function of laser emission power, laser footprint, flight altitude and the reflectivity of the target. While surface reflectivity cannot be controlled, laser power can be increased and low flight altitudes can be maintained.
3. Reduced Scan Angle: Edge-of-scan data can become inaccurate. The scan angle was reduced to a maximum of $\pm 13^{o}$- $\pm 14^{o}$ from nadir (depending on laser system used), creating a narrow swath width and greatly reducing laser shadows from trees and buildings.
4. Quality GPS: Flights took place during optimal GPS conditions (e.g., 6 or more satellites and PDOP [Position Dilution of Precision] less than 3.0). Before each flight, the PDOP was determined for the survey day. During all flight times, two (2) dual frequency DGPS base stations recording at 1–second epochs were utilized and a maximum baseline length between the aircraft and the control points was less than 31 km (20 miles) at all times.
5. Ground Survey: Ground survey point accuracy (i.e., <1.5 cm RMSE) occurs during optimal PDOP ranges and targets a minimal baseline distance of 4 miles between GPS rover and base. Robust statistics are, in part, a function of sample size (n) and distribution. The ground survey collected a total of 6,168 RTK points (covering all study areas) distributed throughout multiple flight lines.
6. 50% Side-Lap (100% Overlap): Overlapping areas are optimized for relative accuracy testing. Laser shadowing is minimized to help increase target acquisition from multiple scan angles. Ideally, with a 50% side-lap, the most nadir portion of one flight line coincides with the edge (least nadir) portion of overlapping flight lines. A minimum of 50% side-lap with terrain-followed acquisition prevents data gaps.
7. Opposing Flight Lines: All overlapping flight lines are opposing. Pitch, roll and heading errors are amplified by a factor of two relative to the adjacent flight line(s), making misalignments easier to detect and resolve.

Relative Accuracy Calibration Methodology

1. Manual System Calibration: Calibration procedures for each mission require solving geometric relationships that relate measured swath-to-swath deviations to misalignments of system attitude parameters. Corrected scale, pitch, roll and heading offsets are calculated and applied to resolve misalignments. The raw divergence between lines is computed after the manual calibration is completed and reported for each study area.

2. Automated Attitude Calibration: All data are tested and calibrated using TerraMatch automated sampling routines. Ground points are classified for each individual flight line and used for line-to-line testing. The resulting overlapping ground points (per line) total hundreds of millions of points for each study area from which to compute and refine relative accuracy. System misalignment offsets (pitch, roll and heading) and

mirror scale are solved for each individual mission. The application of attitude misalignment offsets (and mirror scale) occurs for each individual mission. The data from each mission are then blended when imported together to form the entire area of interest.

3. Automated Z Calibration: Ground points per line are utilized to calculate the vertical divergence between lines caused by vertical GPS drift. Automated Z calibration is the final step employed for relative accuracy calibration.

Relative accuracy statistics and graphs for all study areas are reported and shown below in **Figures 7-24.**

Figure 7. UPPER OKANOGAN STUDY AREA: Relative accuracy per flight line with overlapping point totals listed as 'n'.

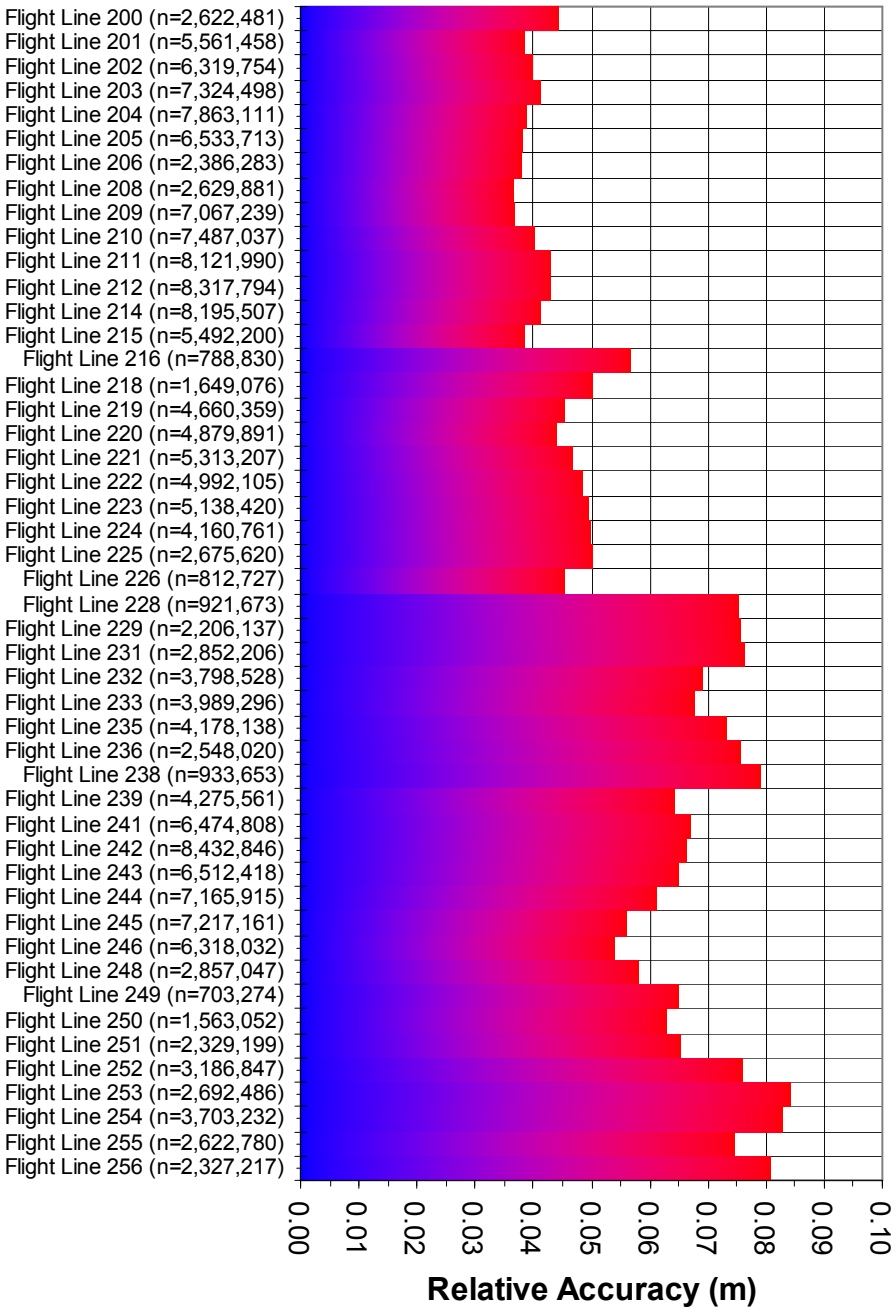

Figure 8. UPPER OKANOGAN STUDY AREA: Distribution of relative accuracies per flight line.

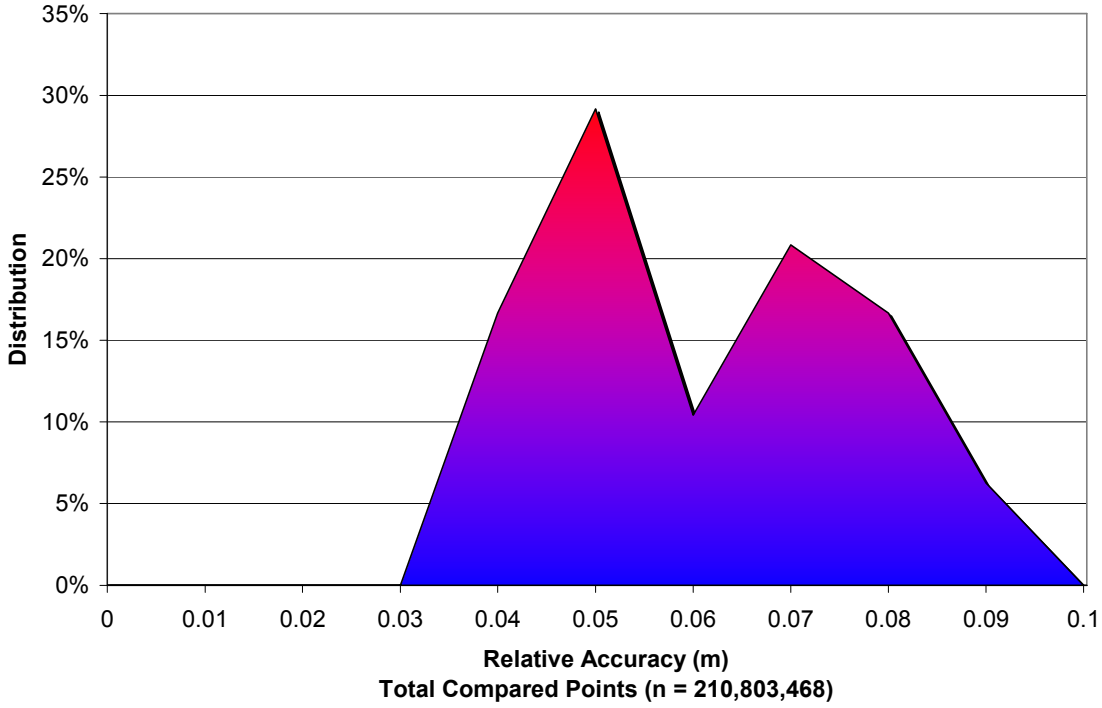

Figure 9. UPPER OKANOGAN STUDY AREA: Statistical relative accuracies.

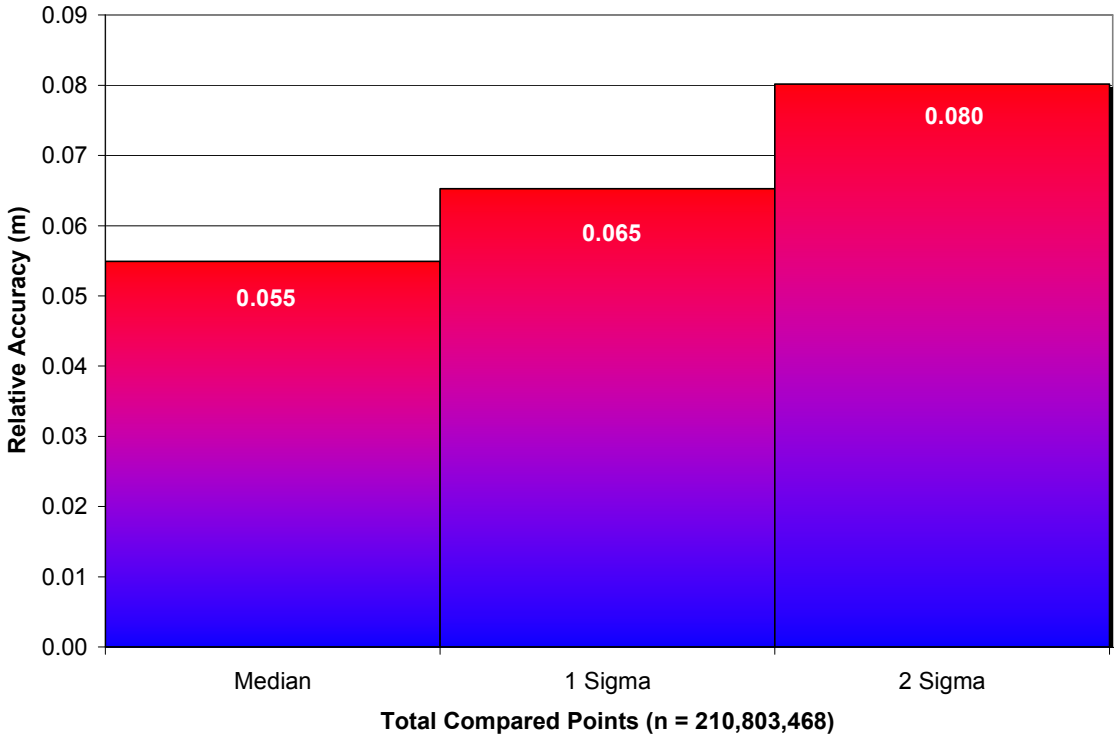

Figure 10. LOWER OKANOGAN STUDY AREA: Relative accuracy per flight line with overlapping point totals listed as 'n'.

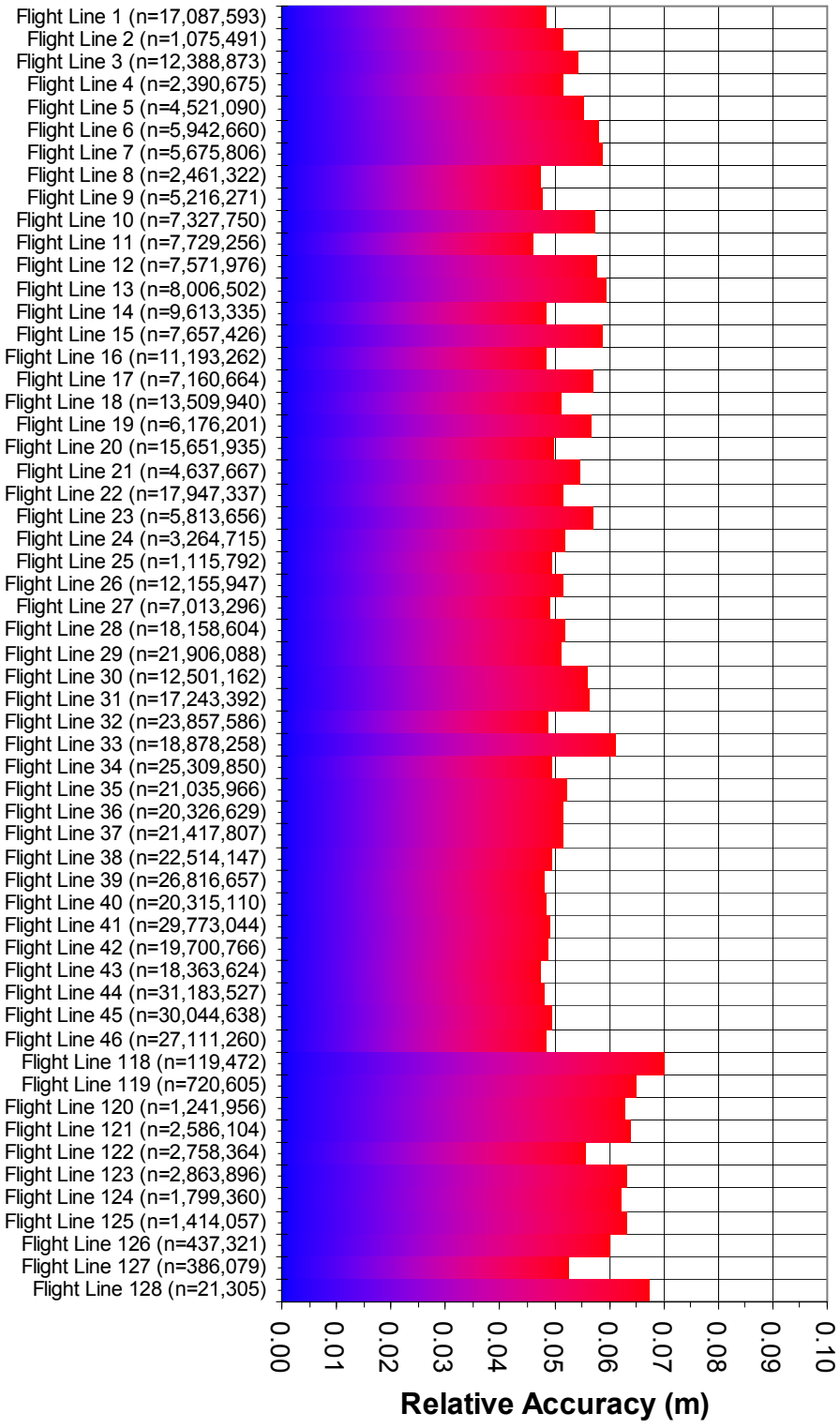

Figure 11. LOWER OKANOGAN STUDY AREA: Distribution of relative accuracies per flight line.

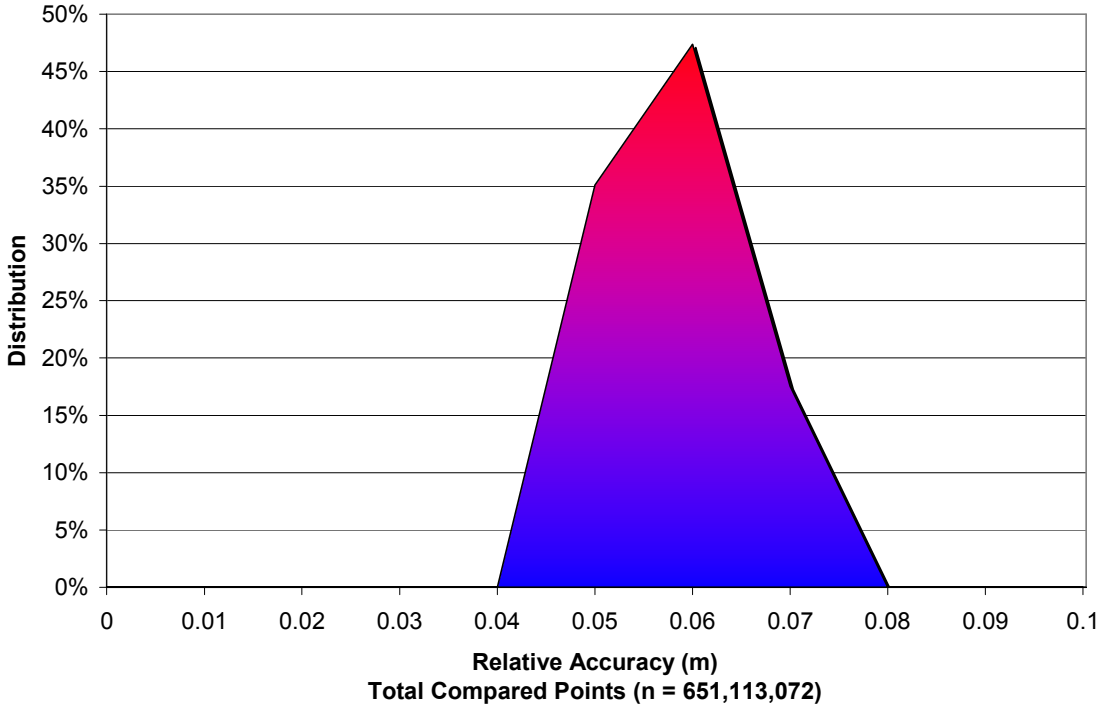

Figure 12. LOWER OKANOGAN STUDY AREA: Statistical relative accuracies.

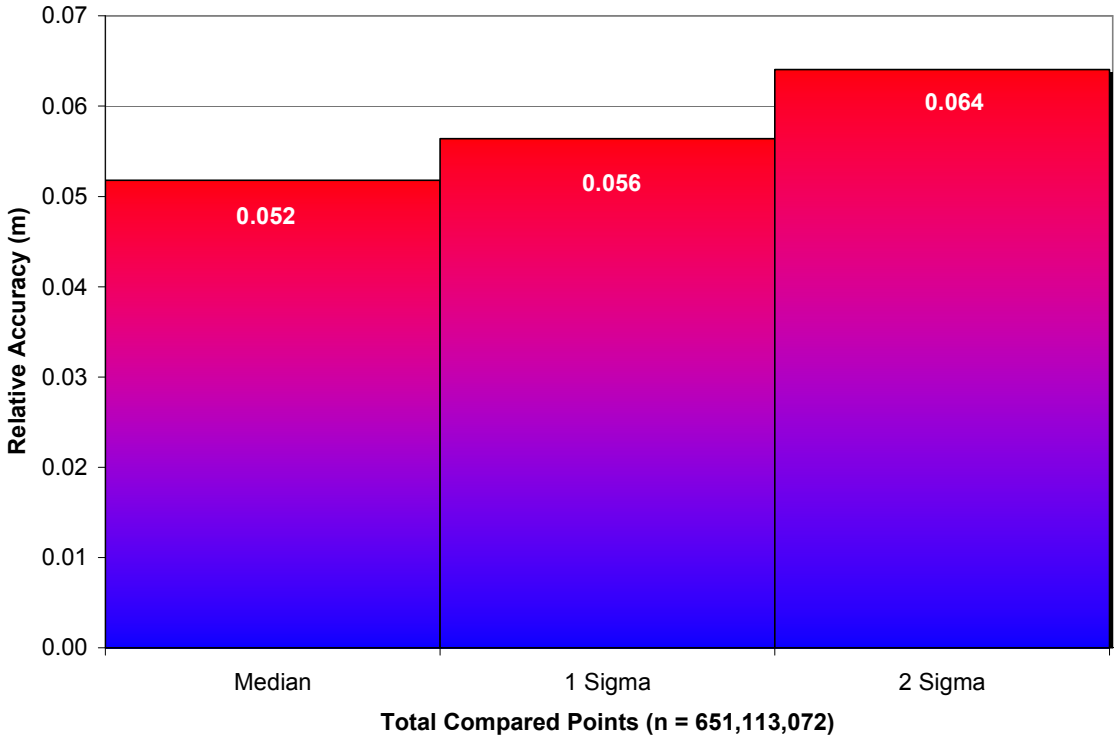

Figure 13. METHOW STUDY AREA: Relative accuracy per flight line with overlapping point totals listed as 'n'.

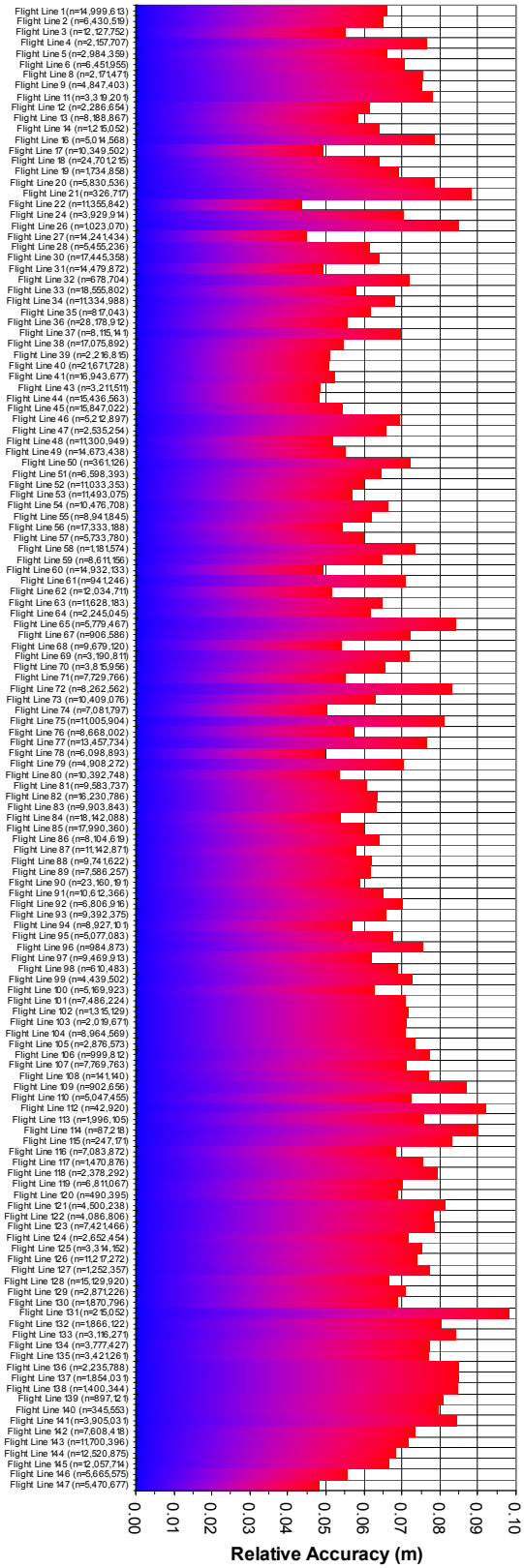

Figure 14. METHOW STUDY AREA: Distribution of relative accuracies per flight line.

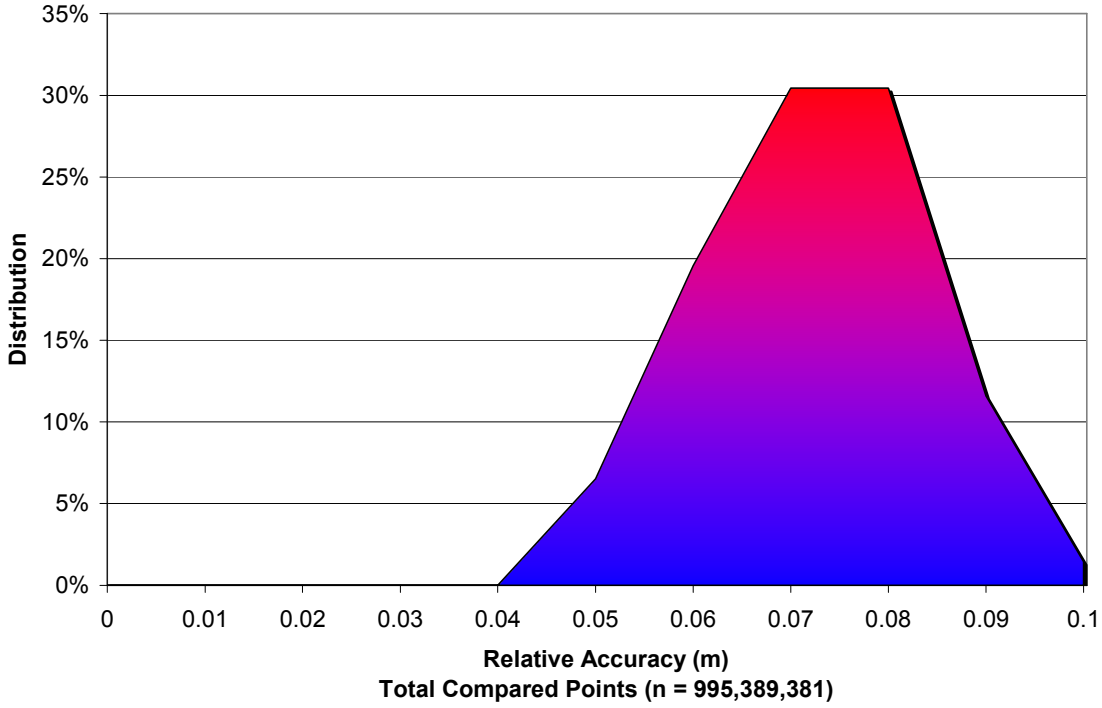

Figure 15. METHOW STUDY AREA: Statistical relative accuracies.

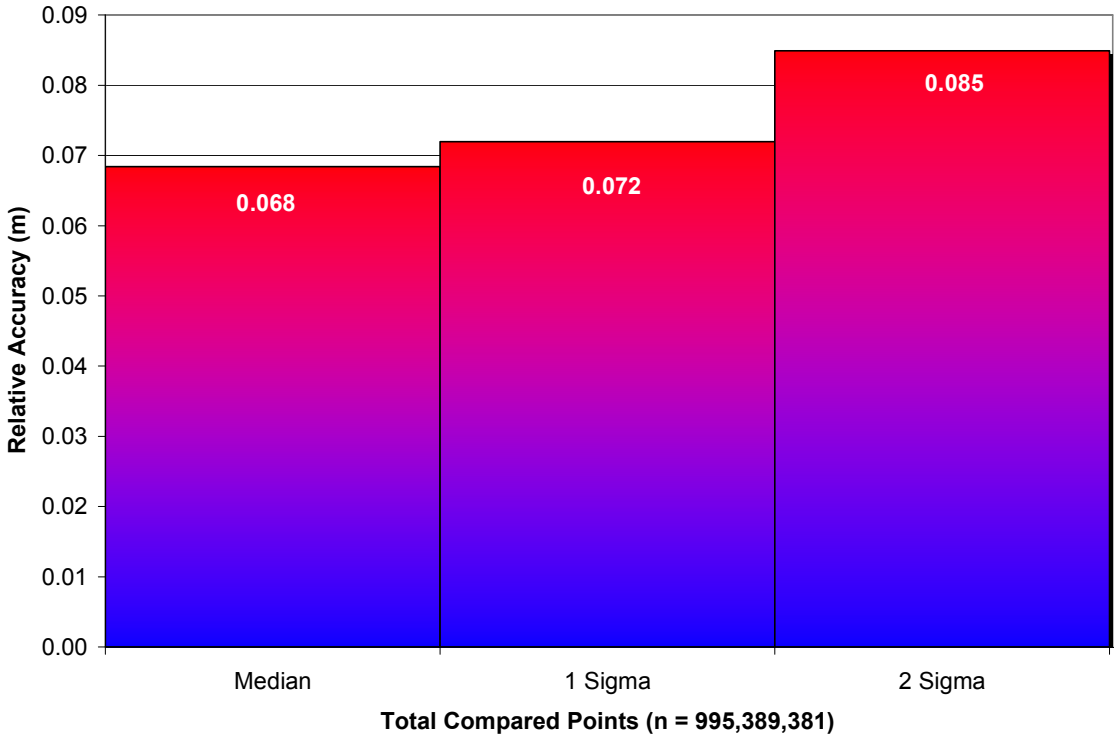

Figure 16. LAKE ROOSEVELT STUDY AREA: Relative accuracy per flight line with overlapping point totals listed as 'n'.

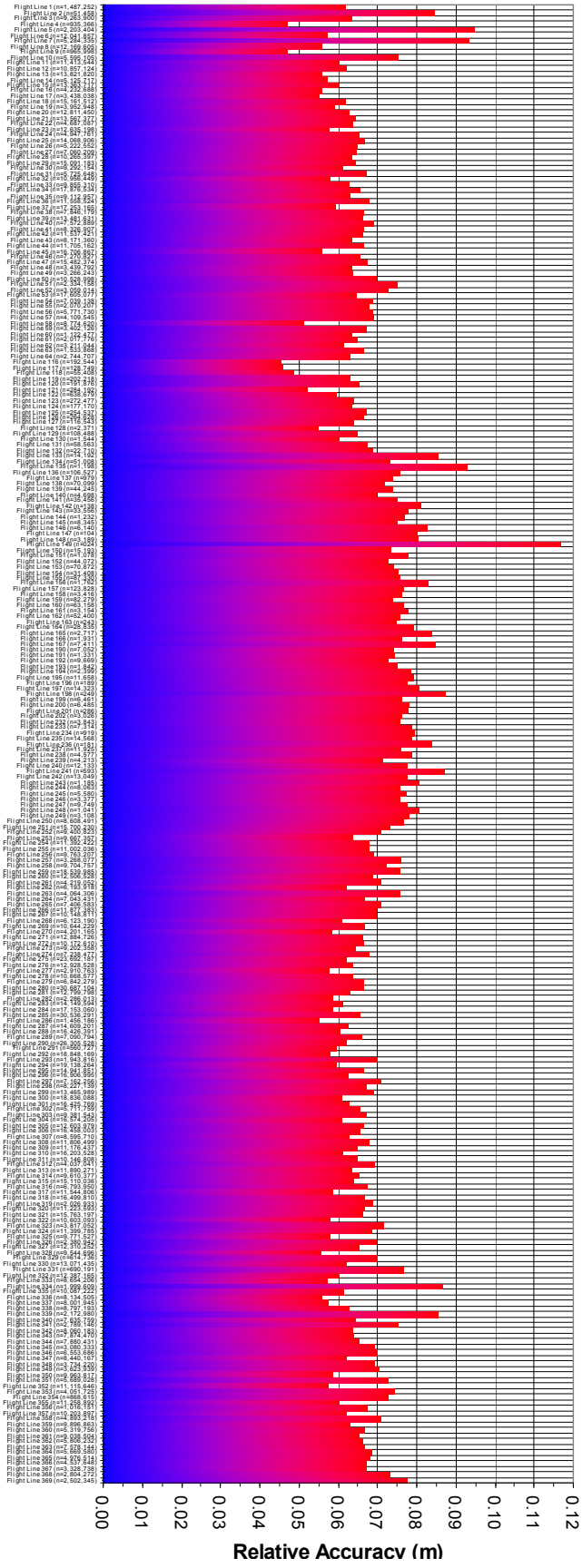

Figure 17. LAKE ROOSEVELT STUDY AREA: Distribution of relative accuracies per flight line.

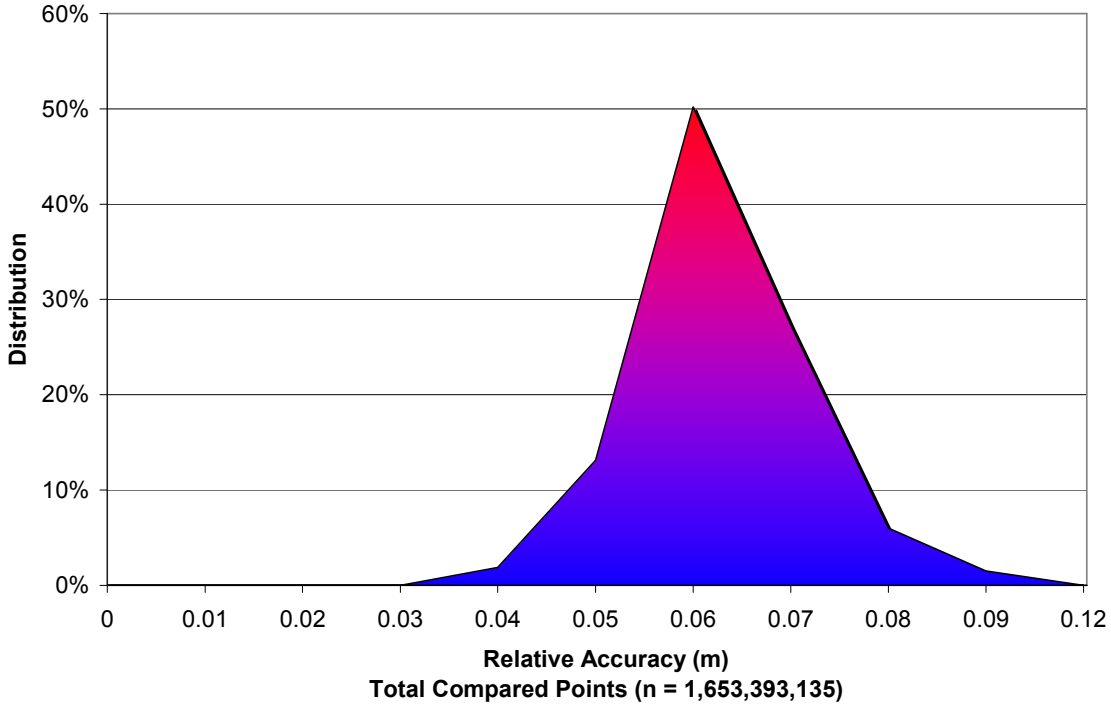

Figure 18. LAKE ROOSEVELT STUDY AREA: Statistical relative accuracies.

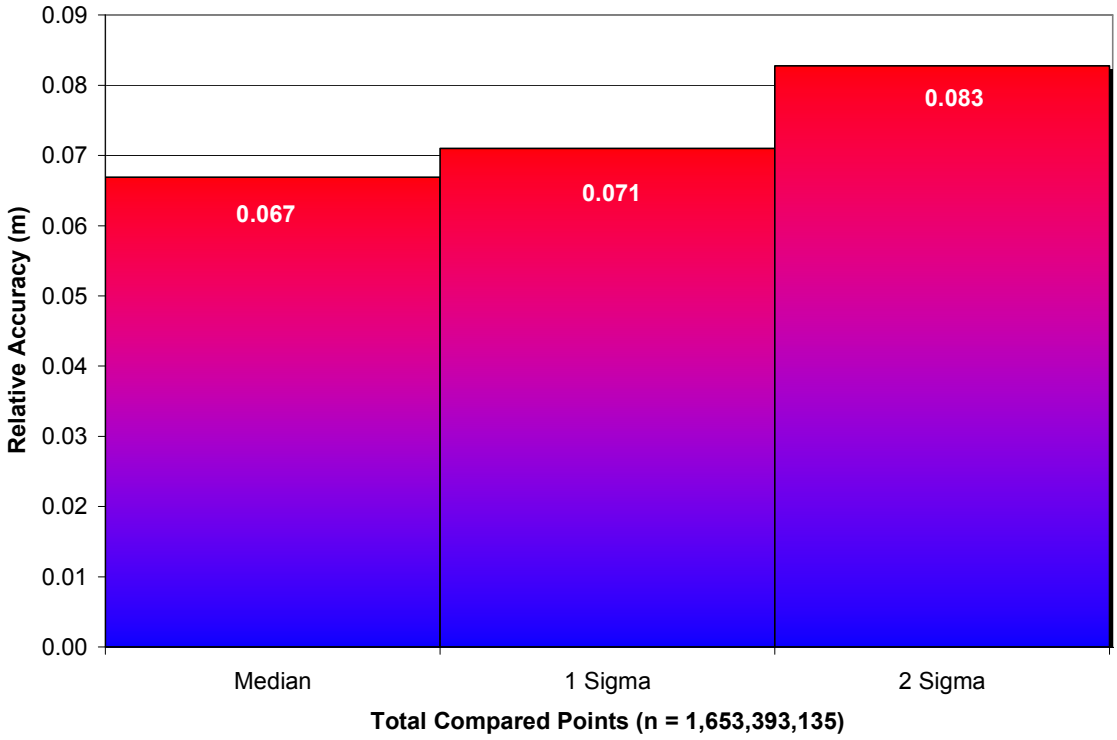

Figure 19. WENATCHEE STUDY AREA: Relative accuracy per flight line with overlapping point totals listed as 'n'.

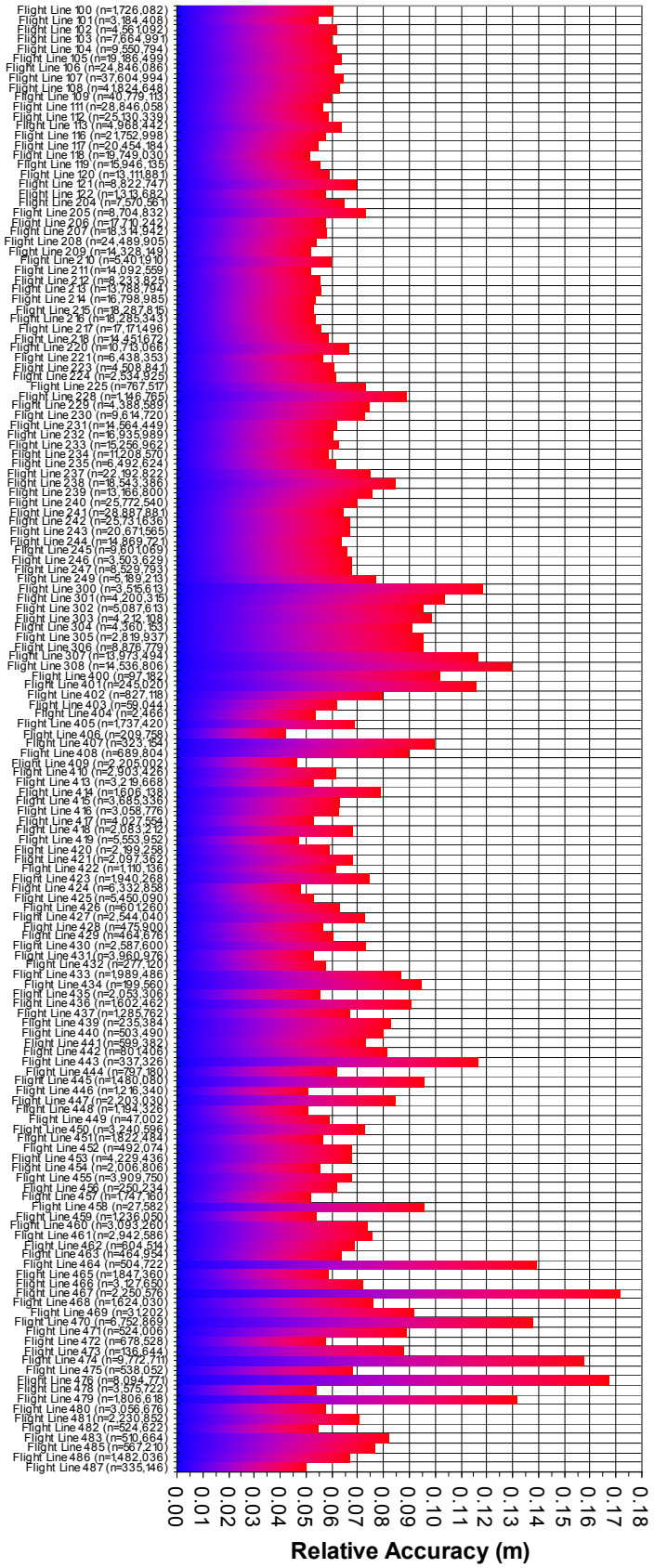

Figure 20. WENATCHEE STUDY AREA: Distribution of relative accuracies per flight line.

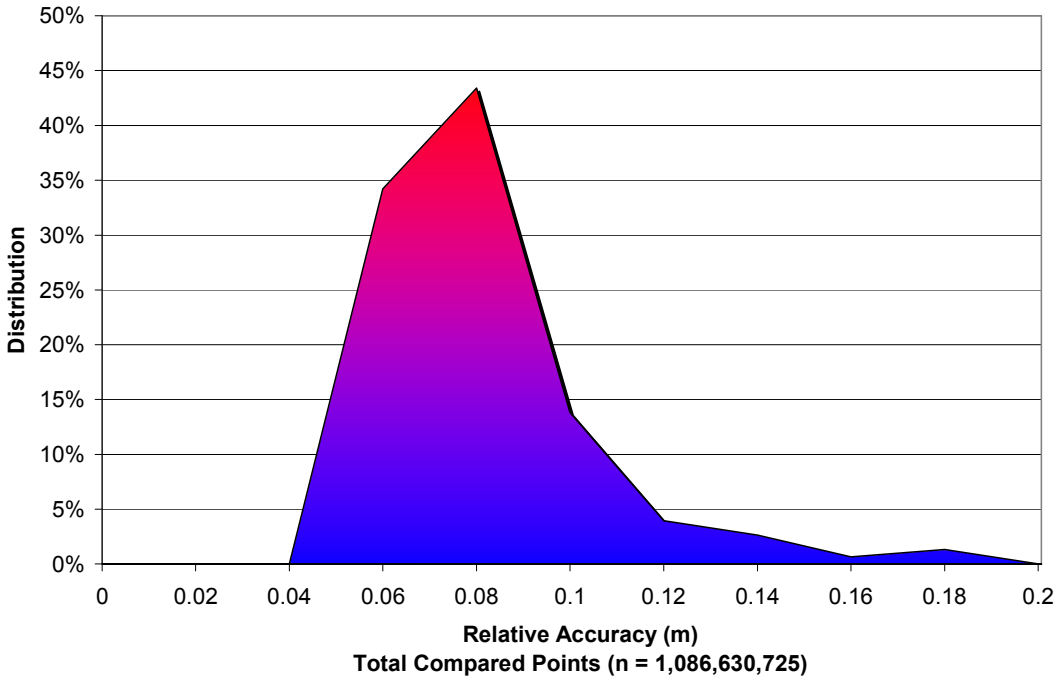

Figure 21. WENATCHEE STUDY AREA: Statistical relative accuracies.

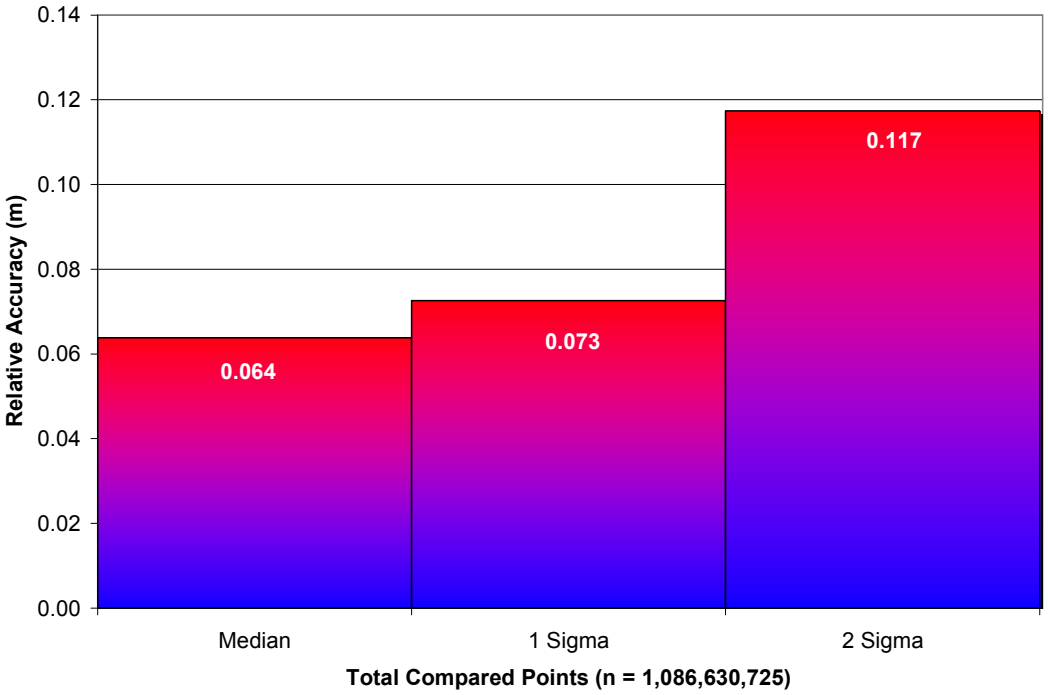

Figure 22. JOHN DAY STUDY AREA: Relative accuracy per flight line with overlapping point totals listed as 'n'.

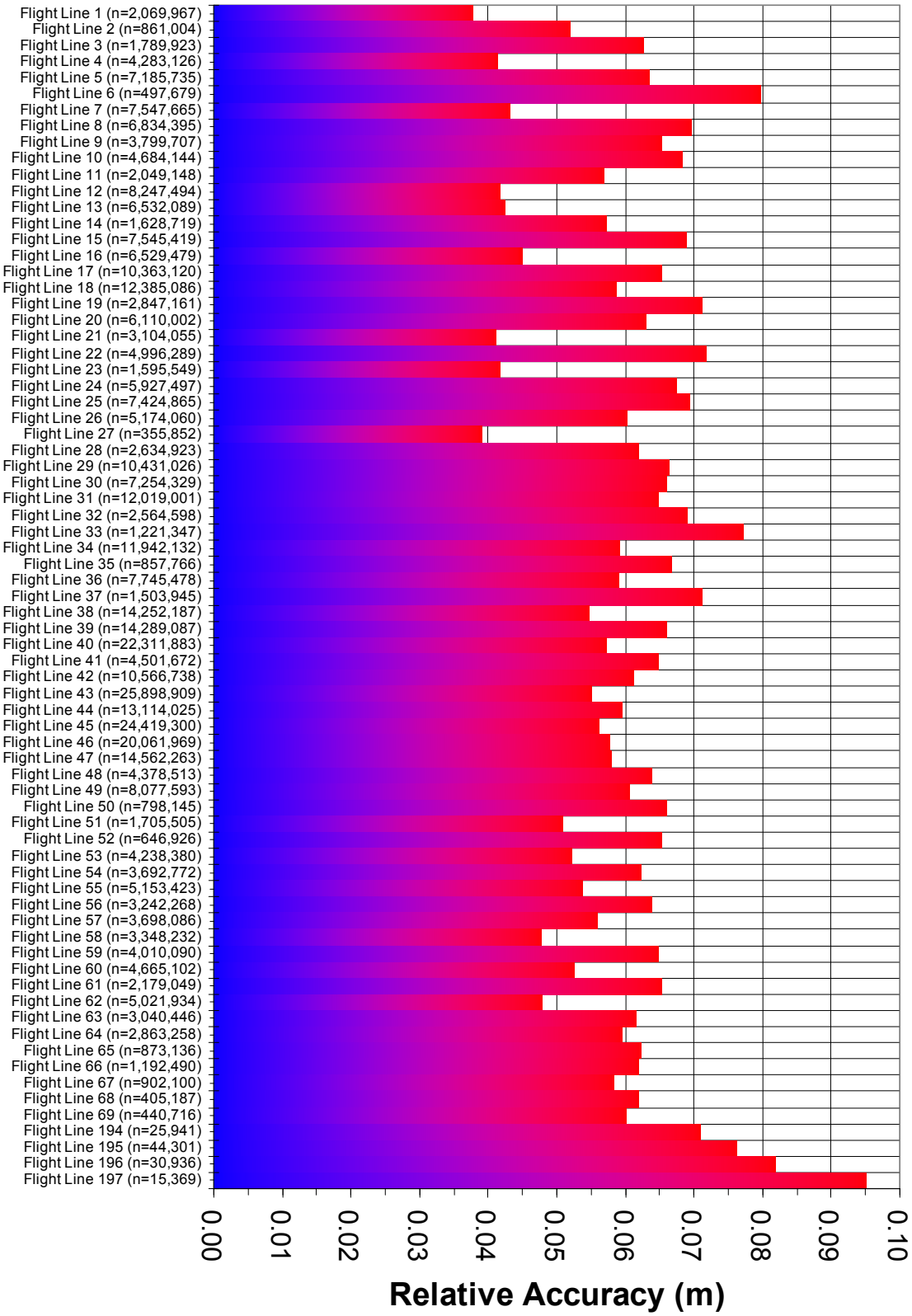

Figure 23. JOHN DAY STUDY AREA: Distribution of relative accuracies per flight line.

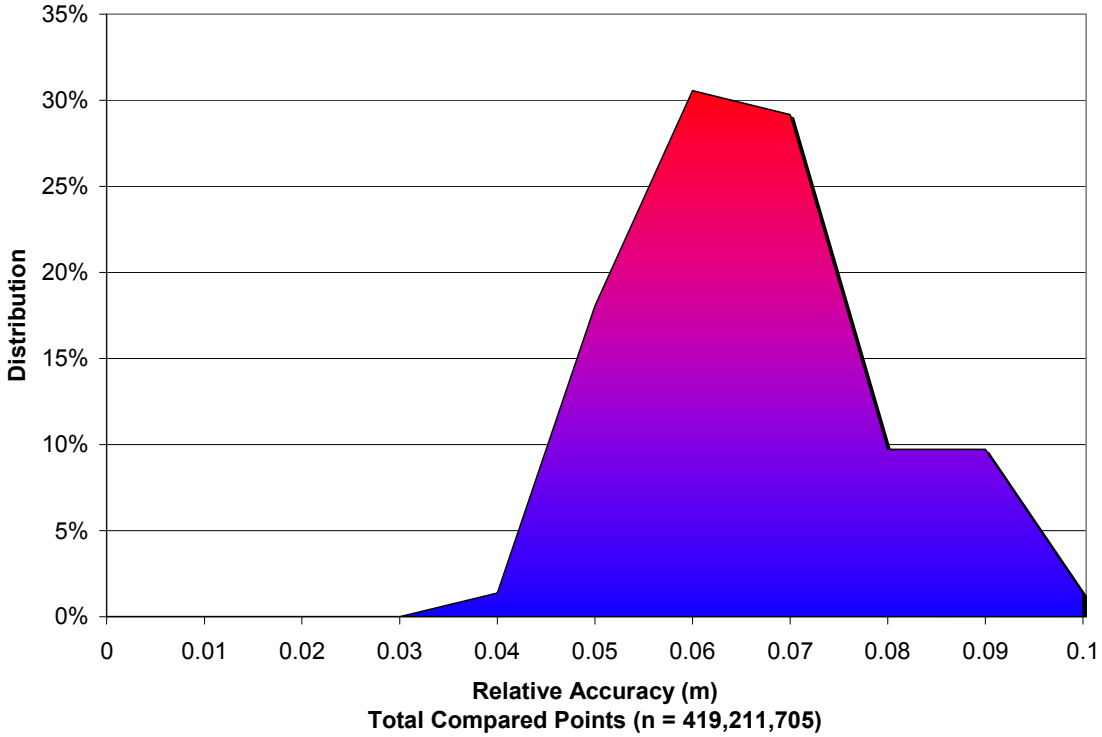

Figure 24. JOHN DAY STUDY AREA: Statistical relative accuracies.

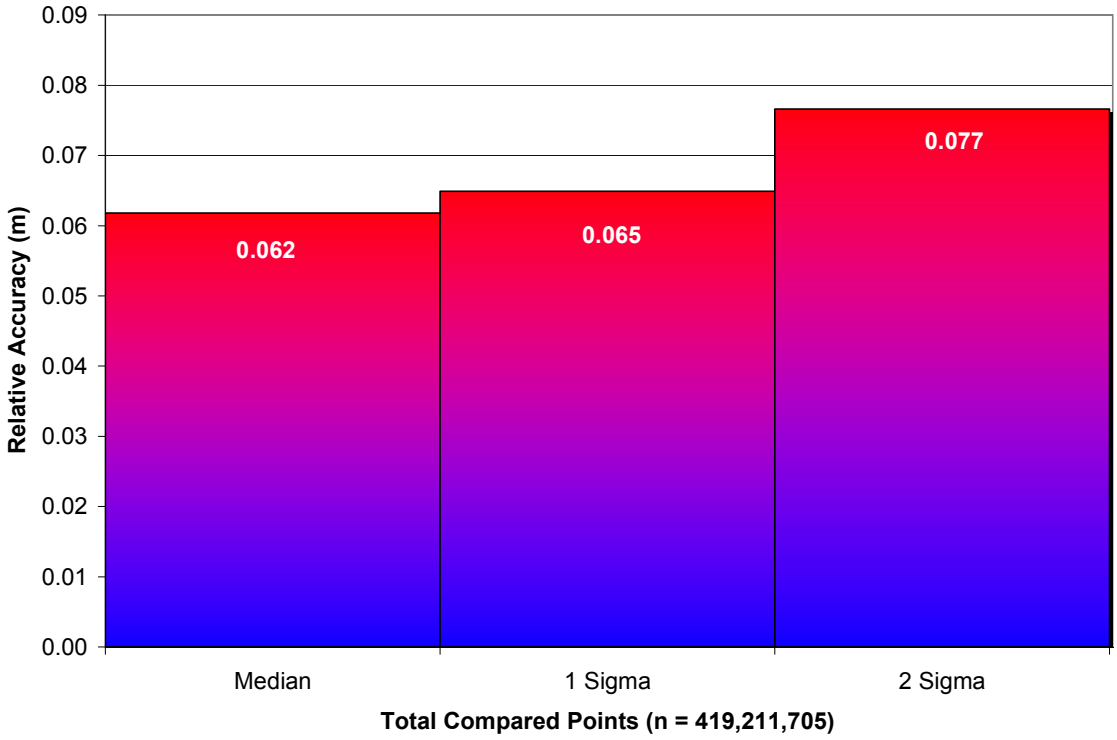

4.1.2 Absolute Accuracy

The final quality control measure is a statistical accuracy assessment that compares known RTK ground survey points to the closest laser point. Accuracy statistics are reported in **Tables 5-10** and shown in **Figures 25-36**.

Table 5. UPPER OKANOGAN STUDY AREA: Absolute Accuracy – Deviation between laser points and RTK survey points.

Sample Size (n): 554	
Root Mean Square Error (RMSE): 0.07 meters	
Standard Deviations	**Deviations**
1 sigma (σ): 0.07 meters	**Minimum Δz:** -0.18 meters
2 sigma (σ): 0.11 meters	**Maximum Δz:** 0.18 meters
	Average Δz: 0.06 meters

Figure 25. UPPER OKANOGAN STUDY AREA: Histogram Statistics

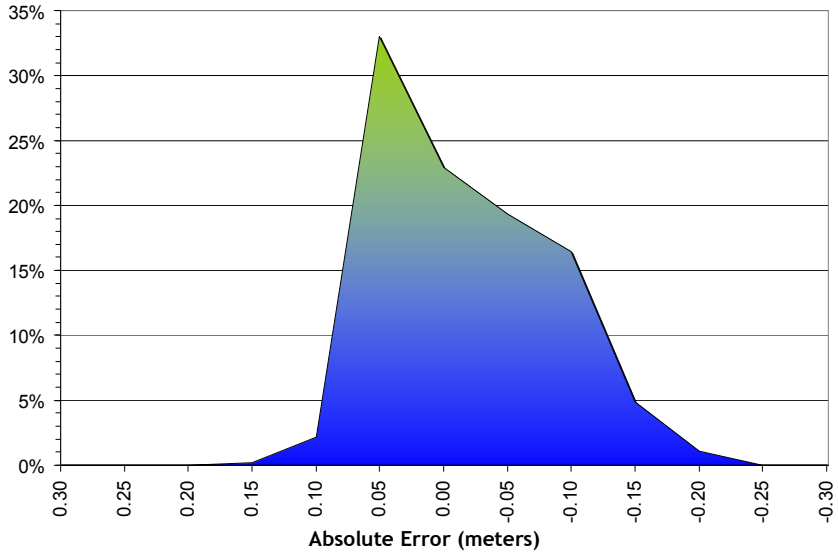

Figure 26. UPPER OKANOGAN STUDY AREA: Point Absolute Deviation Statistics

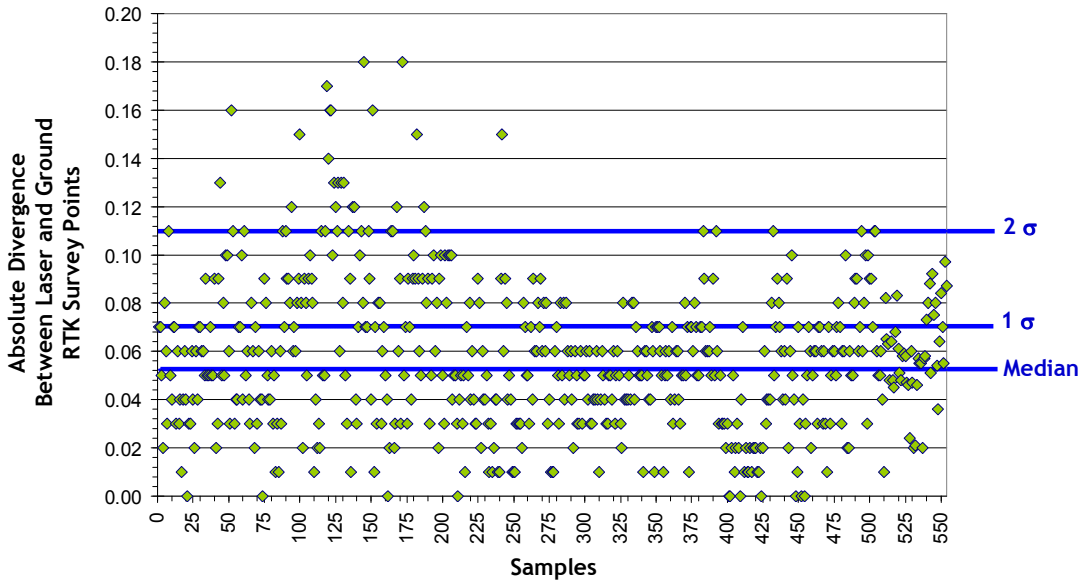

Table 6. LOWER OKANOGAN STUDY AREA: Absolute Accuracy – Deviation between laser points and RTK survey points.

Sample Size (n): 1,152

Root Mean Square Error (RMSE): 0.09 meters

Standard Deviations	Deviations
1 sigma (σ): 0.10 meters	**Minimum Δz:** -0.24 meters
2 sigma (σ): 0.16 meters	**Maximum Δz:** 0.23 meters
	Average Δz: 0.00 meters

Figure 27. LOWER OKANOGAN STUDY AREA: Histogram Statistics

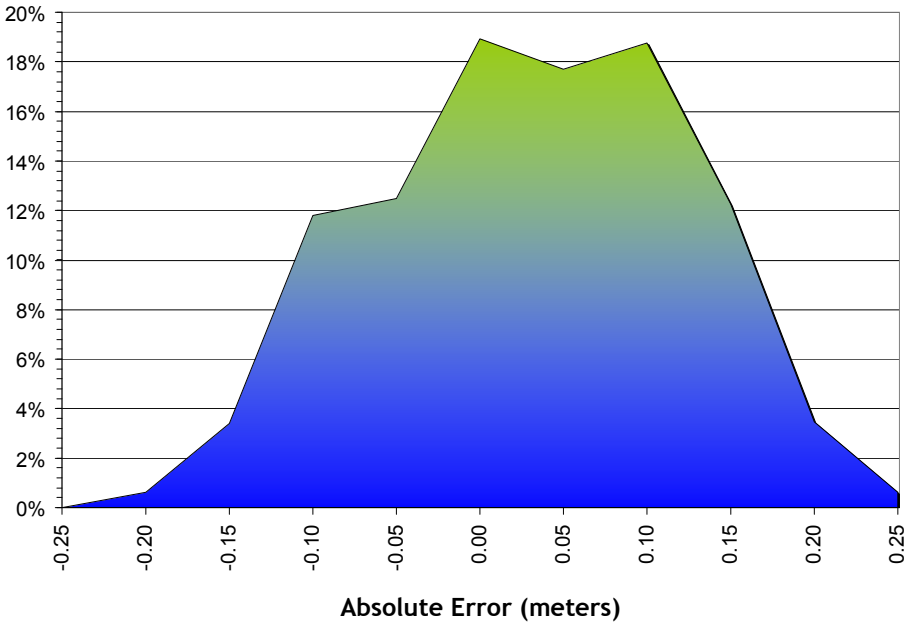

Figure 28. LOWER OKANOGAN STUDY AREA: Point Absolute Deviation Statistics

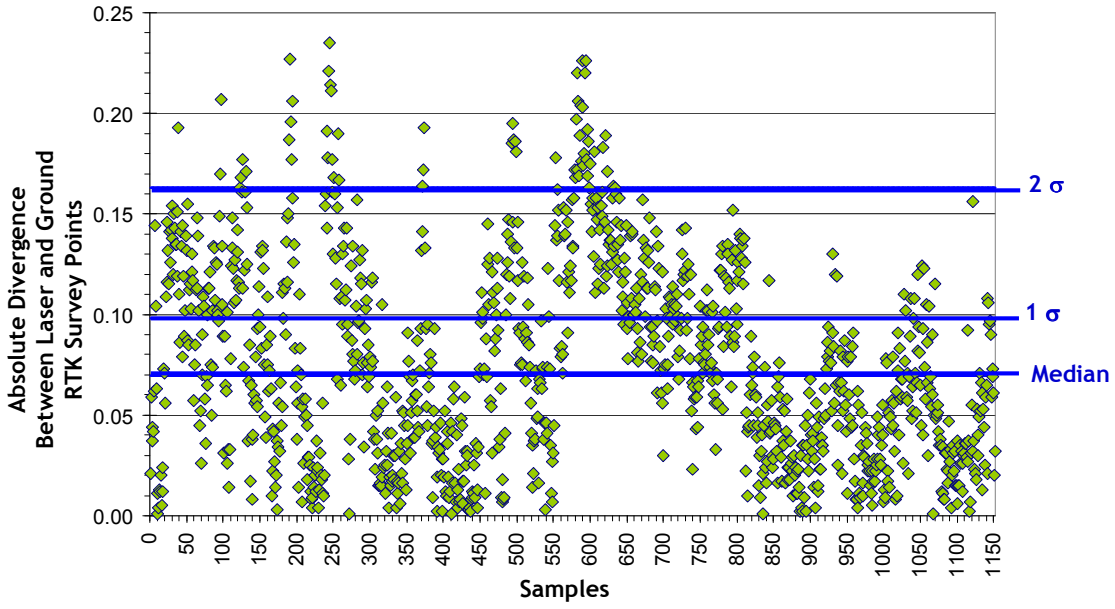

Table 7. METHOW STUDY AREA: Absolute Accuracy – Deviation between laser points and RTK survey points.

Sample Size (n): 555	
Root Mean Square Error (RMSE): 0.09 meters	
Standard Deviations	**Deviations**
1 sigma (σ): 0.10 meters	**Minimum Δz:** -0.16 meters
2 sigma (σ): 0.16 meters	**Maximum Δz:** 0.26 meters
	Average Δz: 0.01 meters

Figure 29. METHOW STUDY AREA: Histogram Statistics

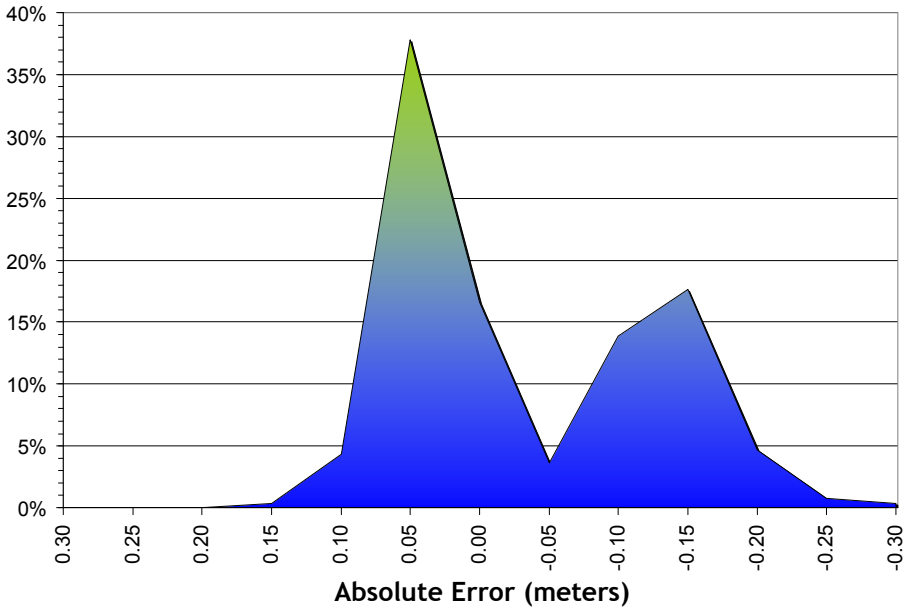

Figure 30. METHOW STUDY AREA: Point Absolute Deviation Statistics

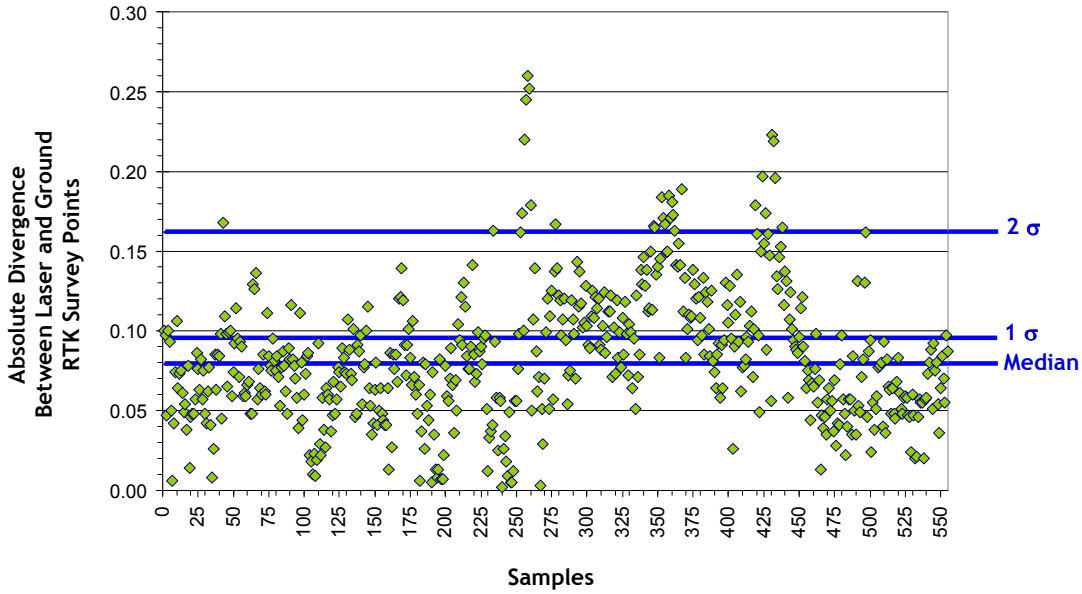

Table 8. LAKE ROOSEVELT STUDY AREA: Absolute Accuracy – Deviation between laser points and RTK survey points.

Sample Size (n): 1,137

Root Mean Square Error (RMSE): 0.05 meters

Standard Deviations	Deviations
1 sigma (σ): 0.05 meters	**Minimum Δz:** -0.22 meters
2 sigma (σ): 0.09 meters	**Maximum Δz:** 0.22 meters
	Average Δz: 0.05 meters

Figure 31. LAKE ROOSEVELT STUDY AREA: Histogram Statistics

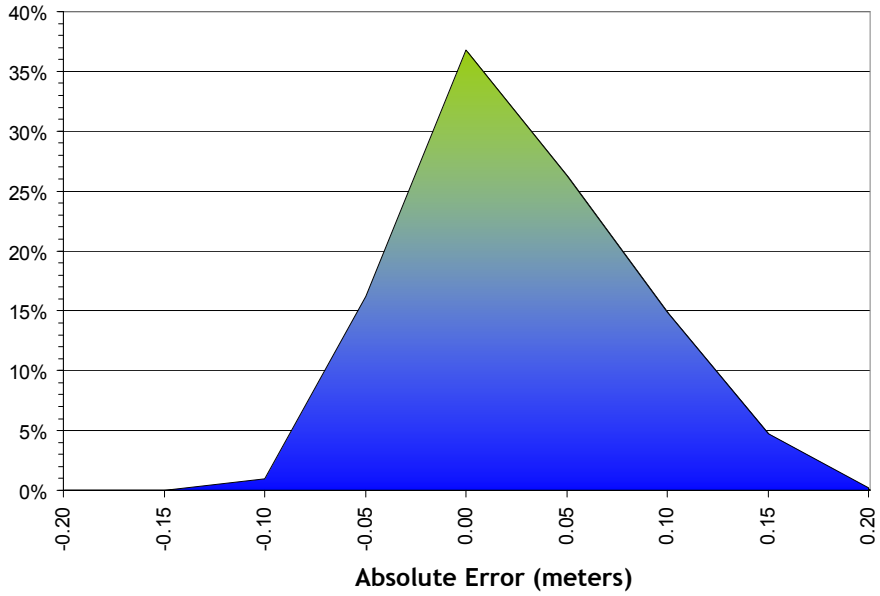

Figure 32. LAKE ROOSEVELT STUDY AREA: Point Absolute Deviation Statistics

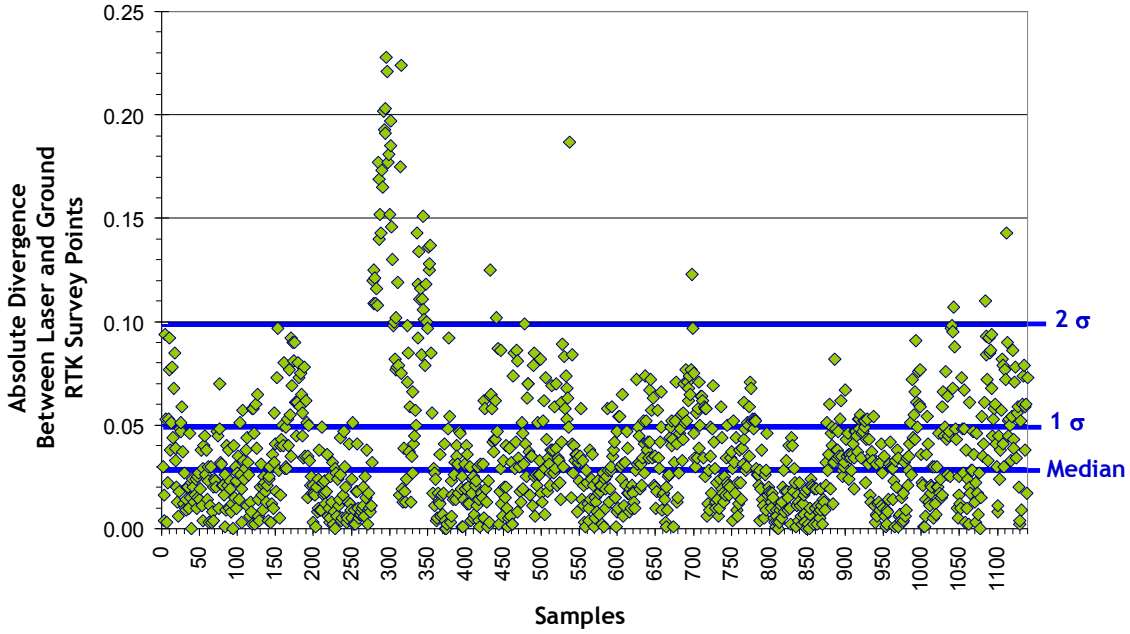

Table 9. WENATCHEE STUDY AREA: Absolute Accuracy – Deviation between laser points and RTK survey points.

Sample Size (n): 562

Root Mean Square Error (RMSE): 0.04 meters

Standard Deviations	Deviations
1 sigma (σ): 0.04 meters	**Minimum Δz:** -0.10 meters
2 sigma (σ): 0.06 meters	**Maximum Δz:** 0.11 meters
	Average Δz: 0.03 meters

Figure 33. WENATCHEE STUDY AREA: Histogram Statistics

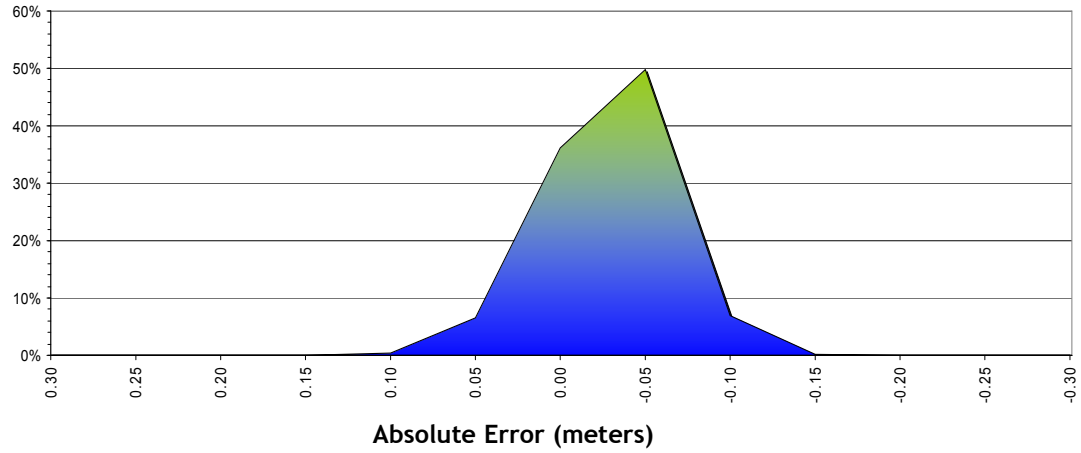

Figure 34. WENATCHEE STUDY AREA: Point Absolute Deviation Statistics

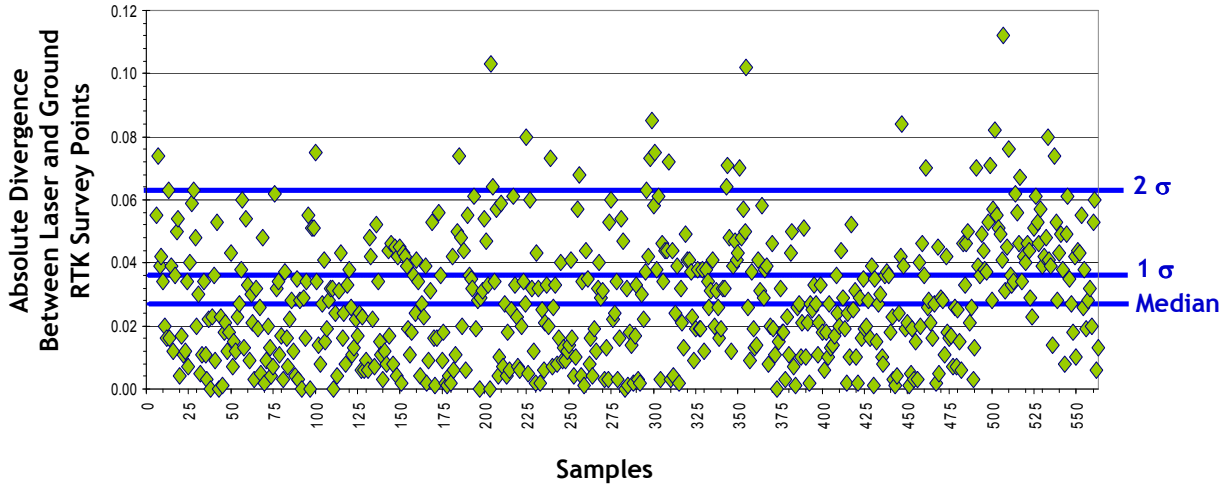

Table 10. JOHN DAY STUDY AREA: Absolute Accuracy – Deviation between laser points and RTK survey points.

Sample Size (n): 1,061	
Root Mean Square Error (RMSE): 0.06 meters	
Standard Deviations	**Deviations**
1 sigma (σ): 0.07 meters	**Minimum Δz:** -0.17 meters
2 sigma (σ): 0.14 meters	**Maximum Δz:** 0.18 meters
	Average Δz: 0.00 meters

Figure 35. JOHN DAY STUDY AREA: Histogram Statistics

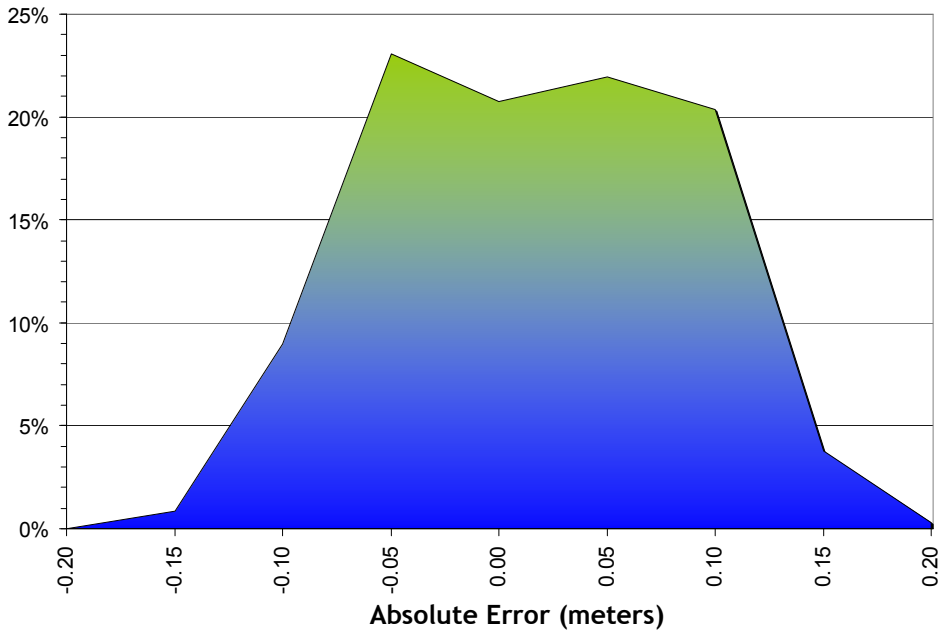

Figure 36. JOHN DAY STUDY AREA: Point Absolute Deviation Statistics

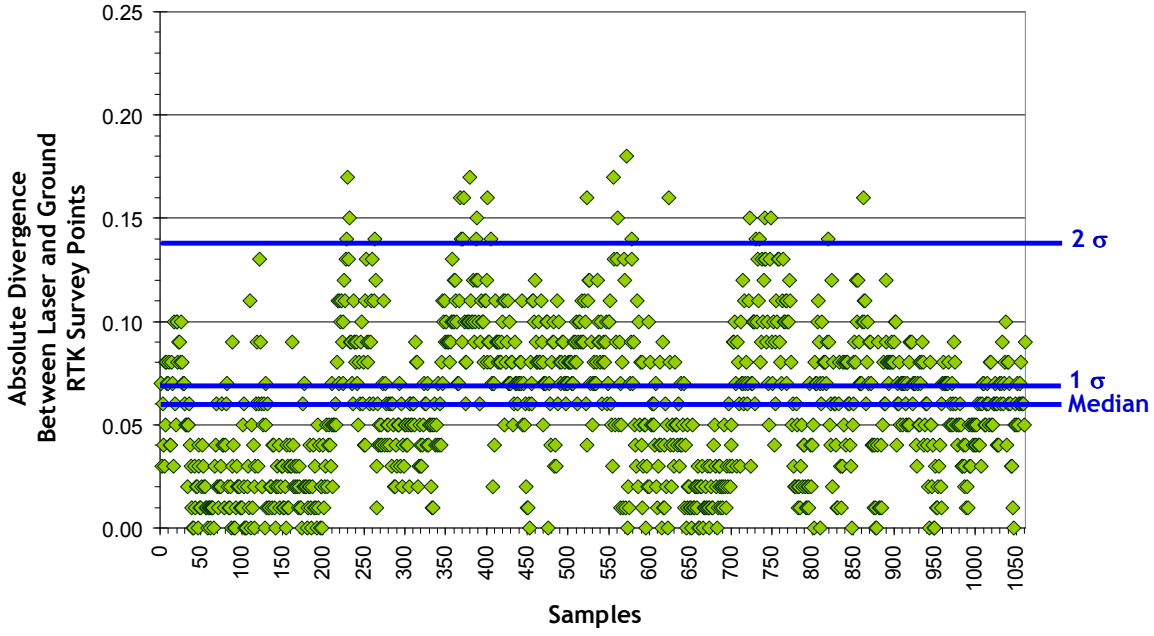

4.2 Datum and Projection

The data were processed as ellipsoidal elevations and required a Geoid transformation to be converted into orthometric elevations (NAVD88). In TerraScan, the NGS published Geiod03 model is applied to each point. The data were processed using meters in the Universal Transverse Mercator (UTM) Zone 10 / 11 (depending on study area) and NAD83 (CORS96)/NAVD88 datum.

5. Deliverables and Specifications

5.1 Point Data (per 0.9375-minute quadrangle ~ 1/64th Quads)

- LAS format V. 1.1
- ASCII space delimited
  Data fields: Number, X, Y, Z, Intensity, ReturnNumber, NumReturns, ScanDirection, EdgeOfFlightLine, Class, SandAngleRank, FileMarker, UserBitField, GPSTime

5.2 Vector Data

- Total Area Flown
  - 7.5-minute and 0.9375-minute quadrangle delineations in shapefile format
- SBET (Smooth Best Estimated Trajectory, 5Hz)
- 0.5-meter (<2-foot) Contour Data (per 0.9375-minute quadrangle ~ 1/64th Quads)
  - AutoCAD Format (*.dwg)

5.3 Raster Data (per 7.5-minute quadrangle)

- ESRI GRIDs of LiDAR dataset:
  - Bare Earth Modeled Points (1-meter resolution),
  - Vegetation Modeled Points- Highest Hit model (1-meter resolution),
- Surface intensity images in GEOTIFF format (Lake Roosevelt at 1-meter resolution; all other study areas at 0.5-meter resolution)

5.4 Data Report

- Full Report containing introduction, methodology, accuracy, and examples
  - Word Format (*.doc)
  - PDF Format (*.pdf)

6. Selected Images

6.1 Plan View Data

An example area is presented to show the following plan view datasets (see **Figures 37-44**):

- Bare earth 1-meter pixel resolution ESRI Grids,
- Contour Data at 0.5-meter intervals,
- Highest Hit vegetation 1-meter resolution ESRI Grids, and
- Intensity GeoTIFFs.

Figure 37. Bare Earth 1-meter resolution ESRI grid showing detail in quad 48119-G4 in the **Lower Okanogan River study area.**

Figure 38. Contour data at 0.5-meter intervals showing detail in quad 48119-G4 in the **Lower Okanogan River study area.**

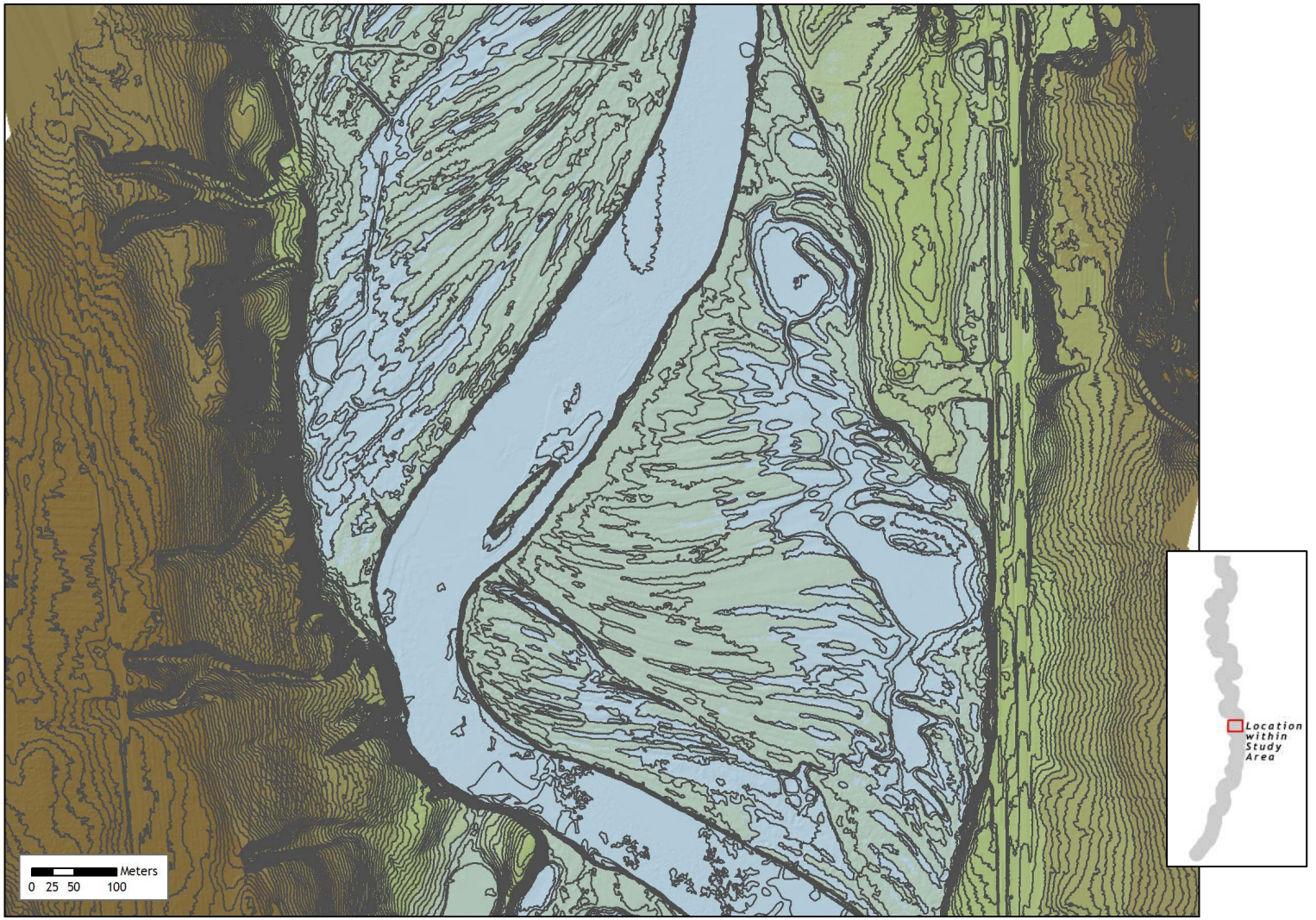

Figure 39. The Highest Hit 1-meter resolution ESRI grid showing detail in quad 48119-G4 in the **Lower Okanogan River study area.**

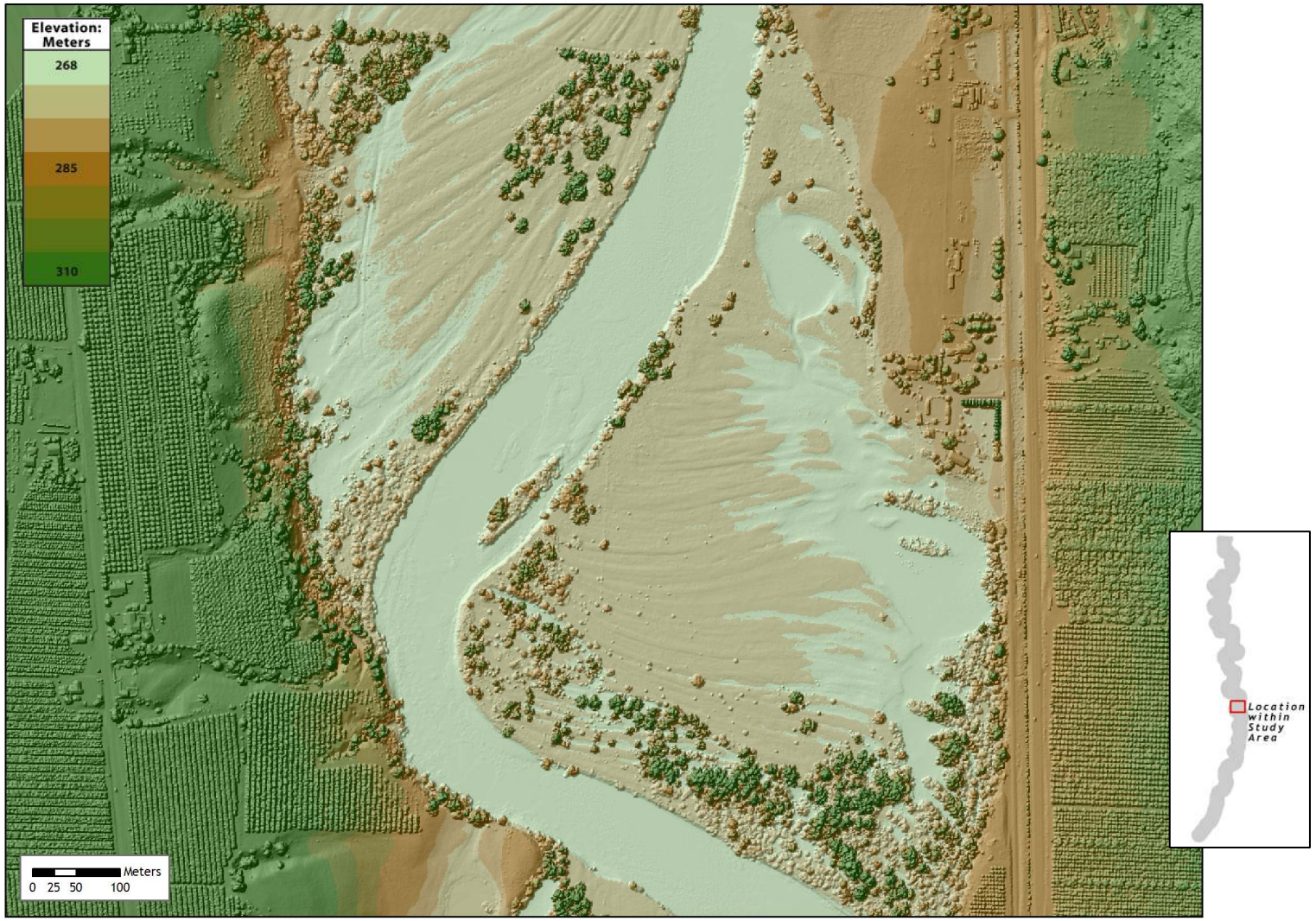

Figure 40. 0.5-meter resolution intensity image showing detail in quad 48119-G4 in the **Lower Okanogan River study area.**

Figure 41. Bare Earth 1-meter resolution ESRI grid showing detail in quad 44118-H7 in the **John Day River study area.**

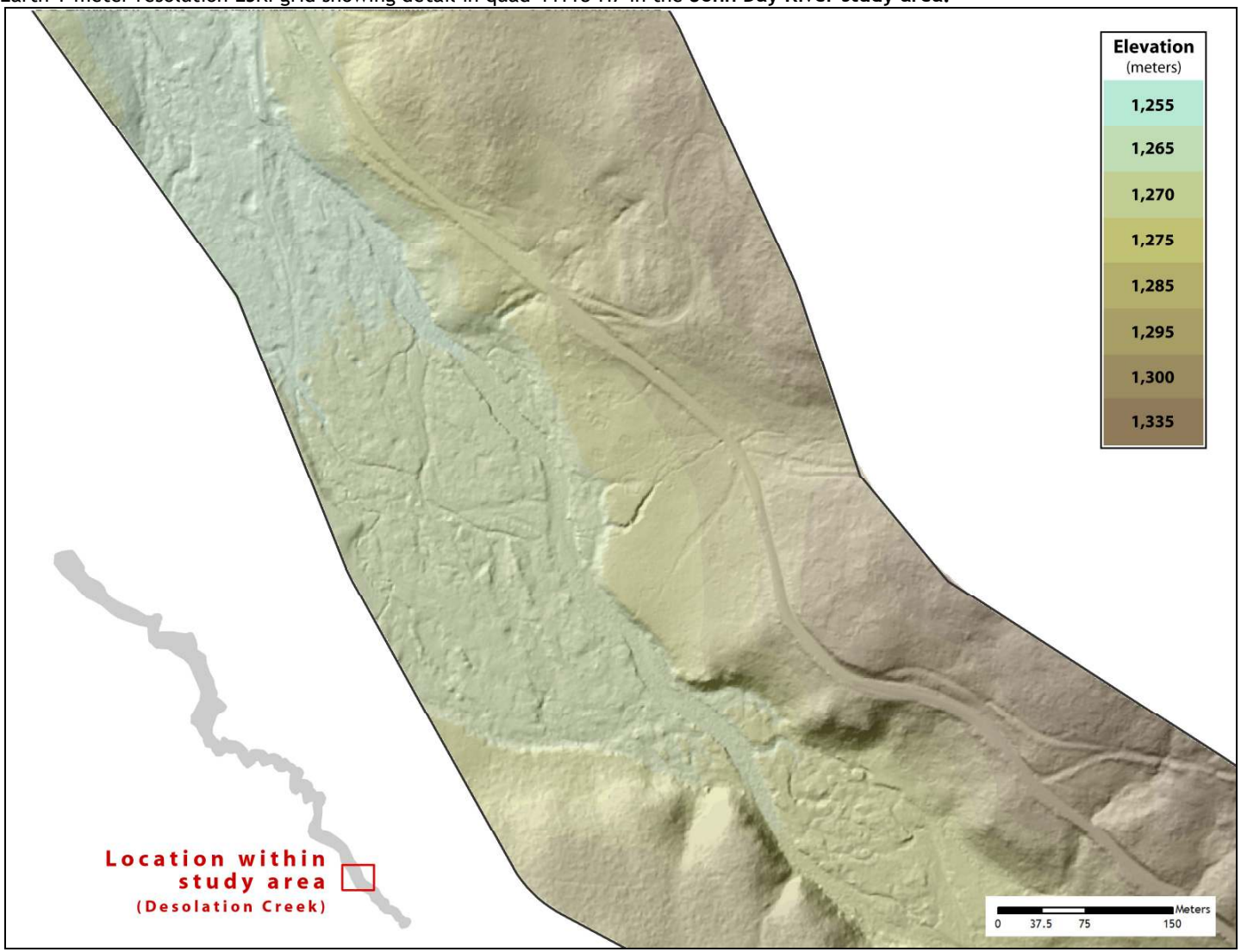

Figure 42. Contour data at 0.5-meter intervals showing detail in quad 44118-H7 in the **John Day River study area.**

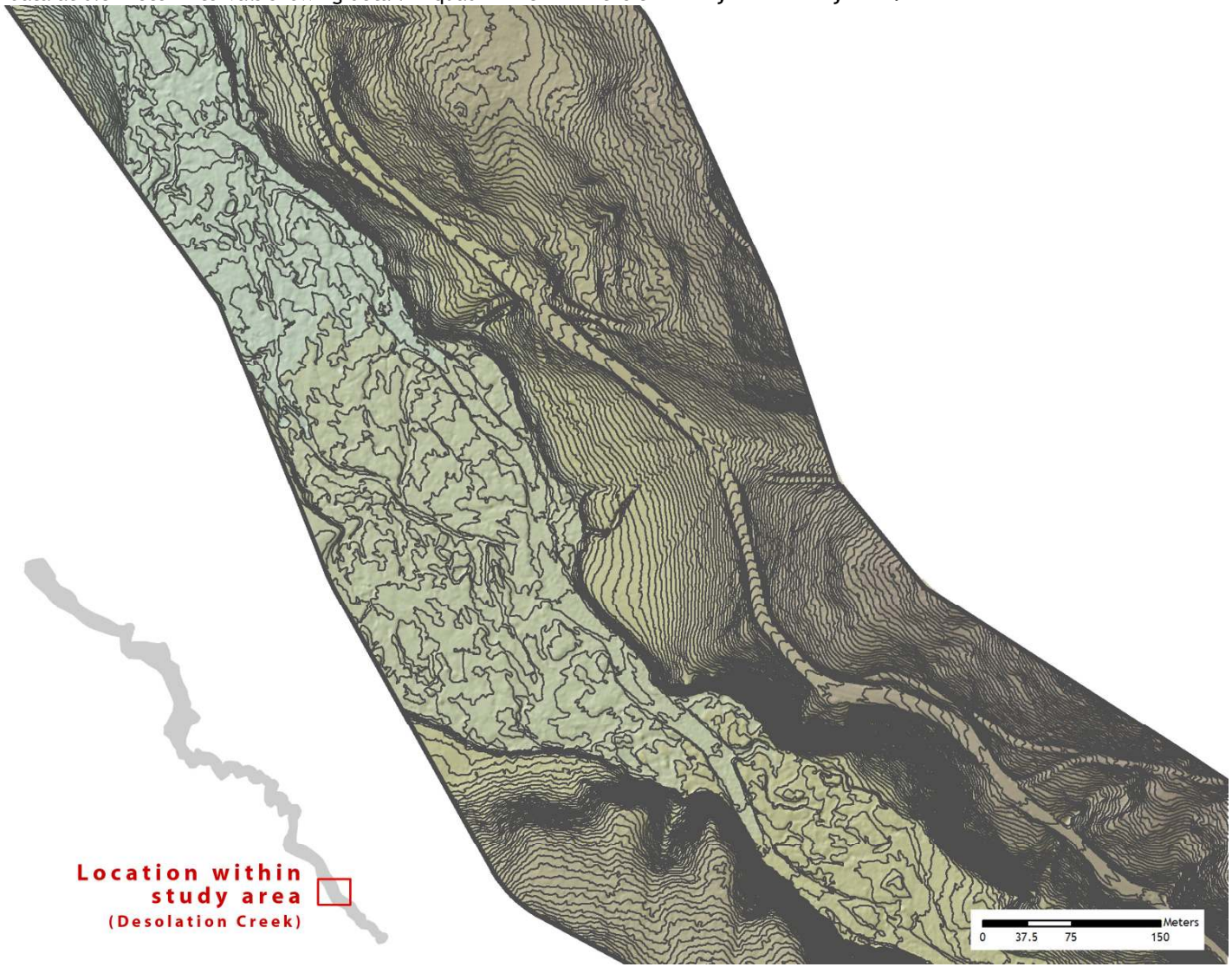

Figure 43. The Highest Hit 1-meter resolution ESRI grid showing detail in quad 44118-H7 in the **John Day River study area.** To calculate vegetation heights, the Bare Earth grid was subtracted from the Highest Hit grid.

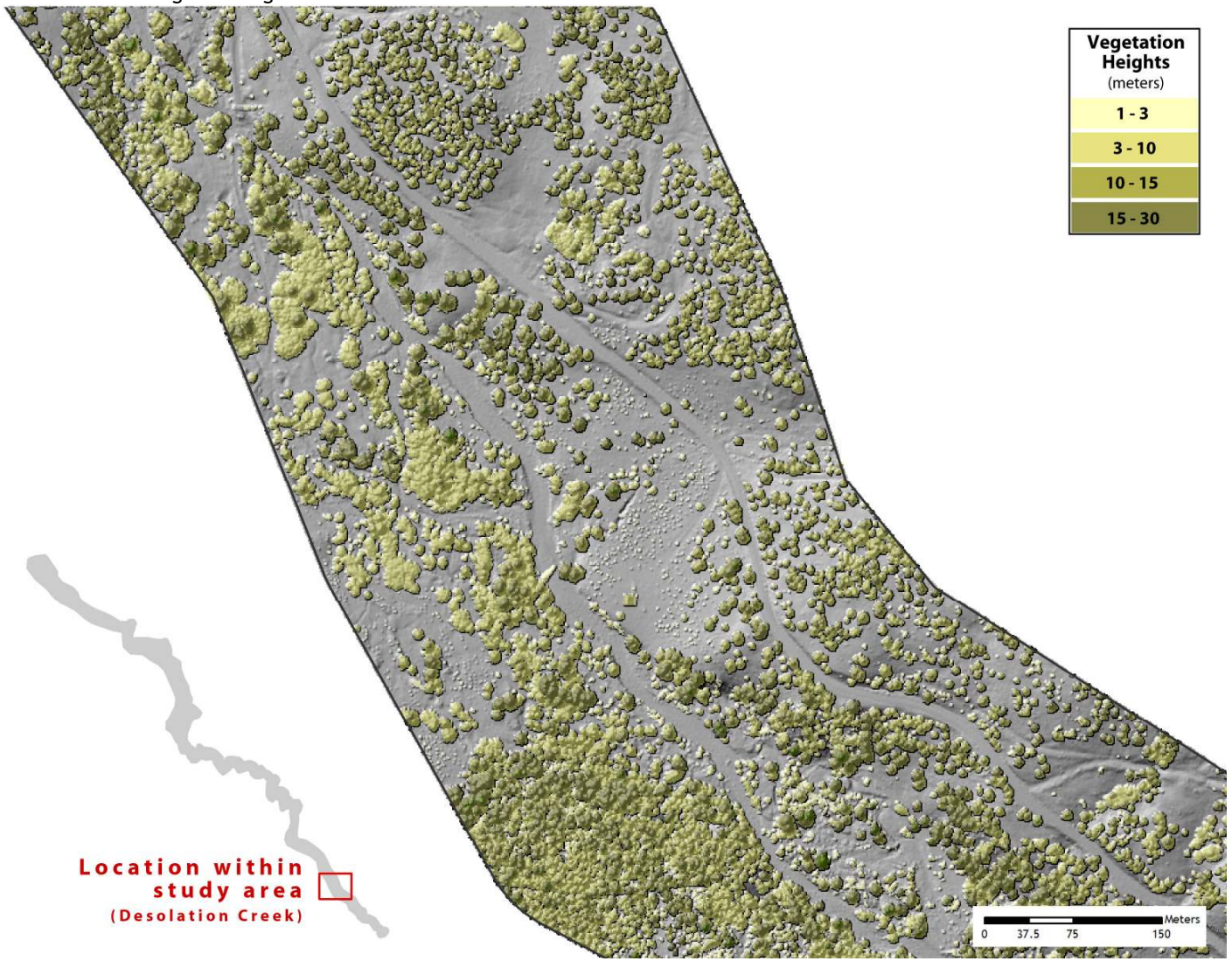

Figure 44. 0.5-meter resolution intensity image showing detail in quad 44118-H7 in the **John Day River study area.**

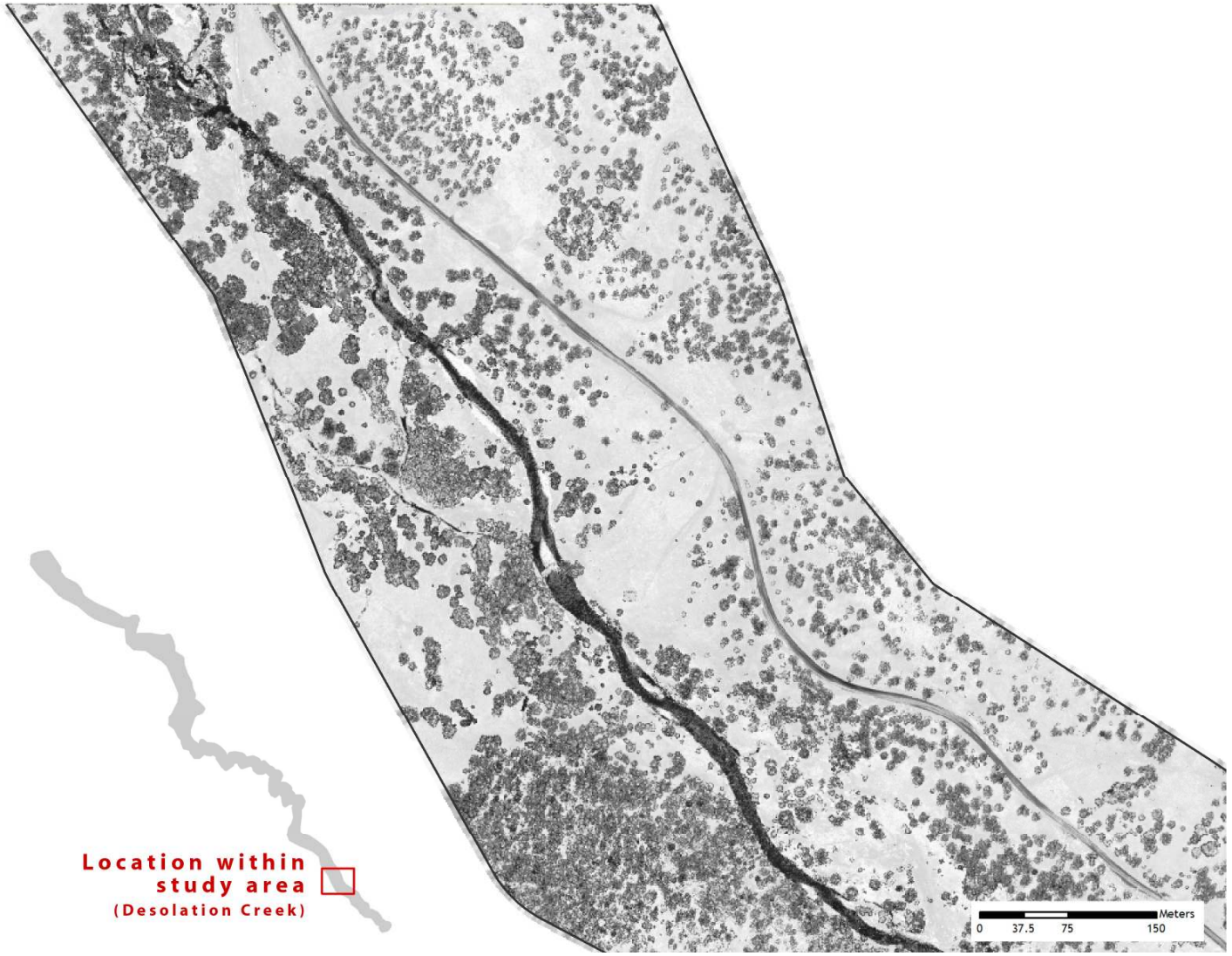

6.2 Three Dimensional Oblique View Data Pairs

Example areas are presented to show paired, same-scene 3-D oblique view imagery (see **Figures 45-58**). These pairs depict a 0.5-meter resolution triangulated irregular network (TIN) model of ground-classified LiDAR points colored by elevation (top image), and a point cloud of all points colored by elevation and intensity shading (bottom image). *Please note that the oblique view images are not always north-oriented.*

Figure 45. 3-d oblique view of LiDAR-derived surfaces in the central portion of quad 49119-D5 along the Okanogan River in the **Upper Okanogan, Canada, study area.** (Top image derived from ground-classified points, bottom image derived from all points).

Figure 46. 3-d oblique view of LiDAR-derived surfaces in the central portion of quad 49119-C4, along Shuttleworth Creek in the **Upper Okanogan, Canada, study area.** (Top image derived from ground-classified points, bottom image derived from all points).

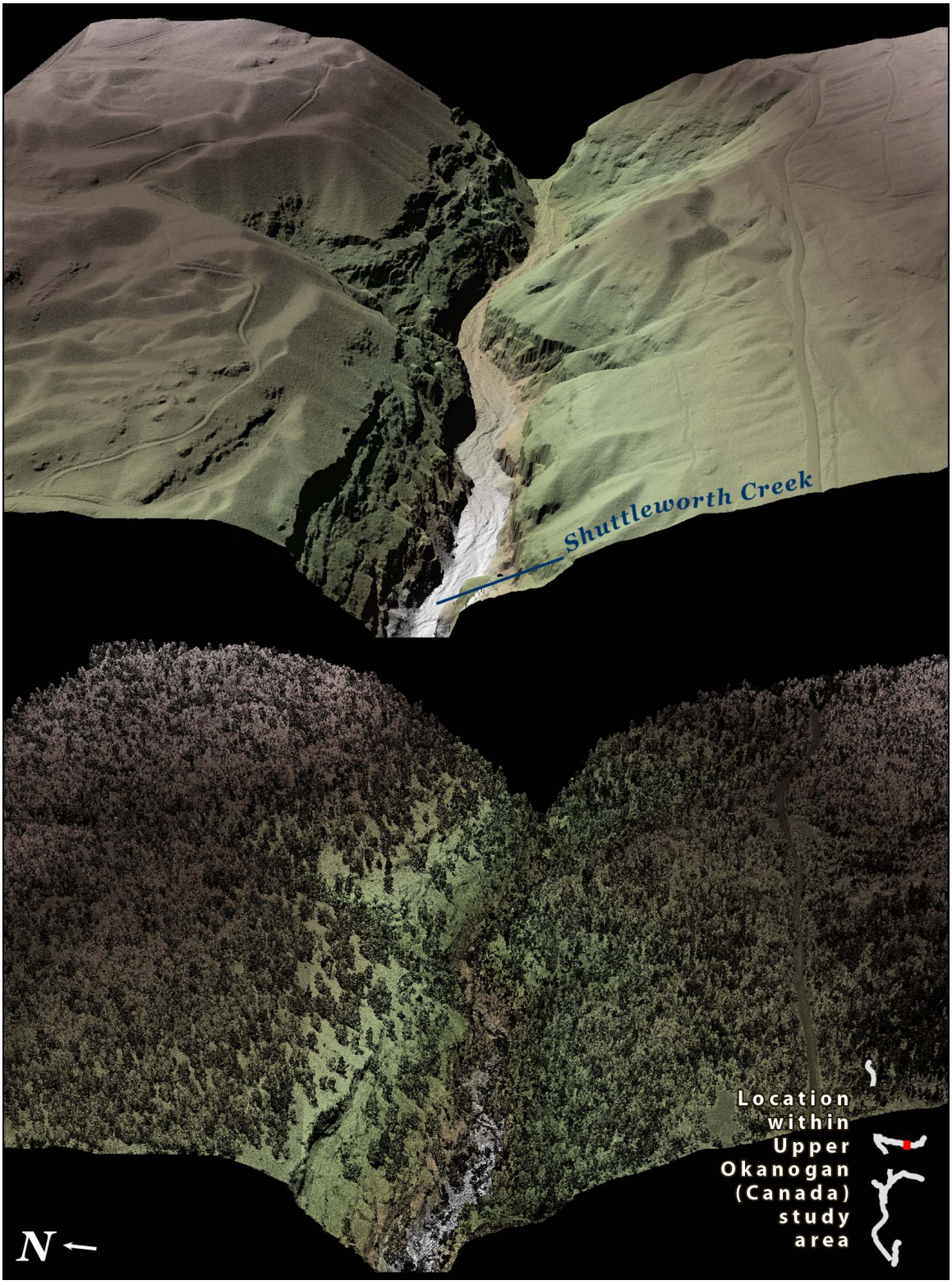

Figure 47. 3-d oblique view of LiDAR-derived surfaces in quad 49119-C5, along the Okanogan River, in the **Upper Okanogan, Canada, study area.** (Top image derived from ground-classified points, bottom image derived from all points).

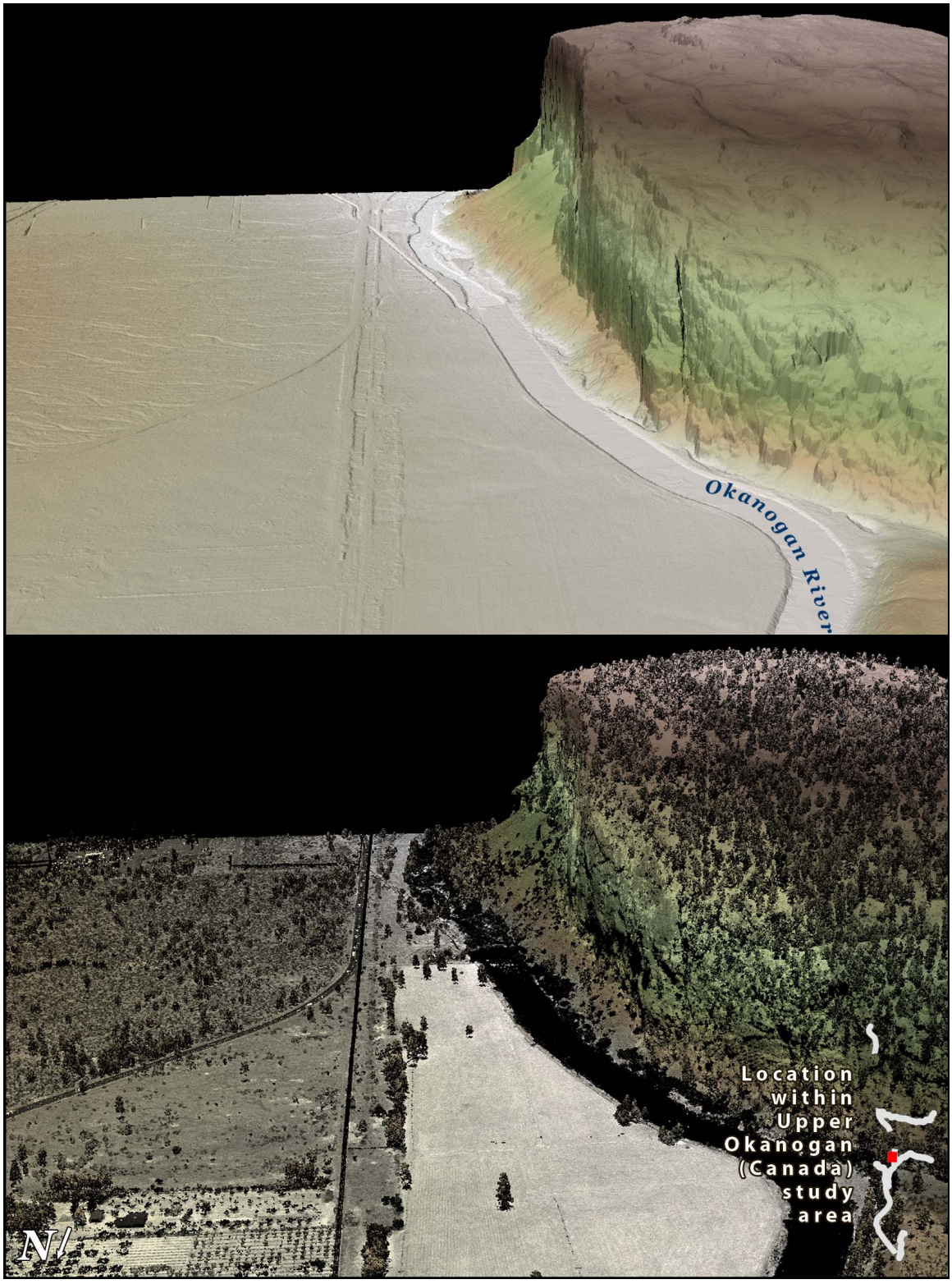

Figure 48. 3-d oblique view of LiDAR-derived surfaces in quad 49119-C5 at the mouth of Vaseux Creek in the **Upper Okanogan, Canada, study area.** (Top image derived from ground-classified points, bottom image derived from all points).

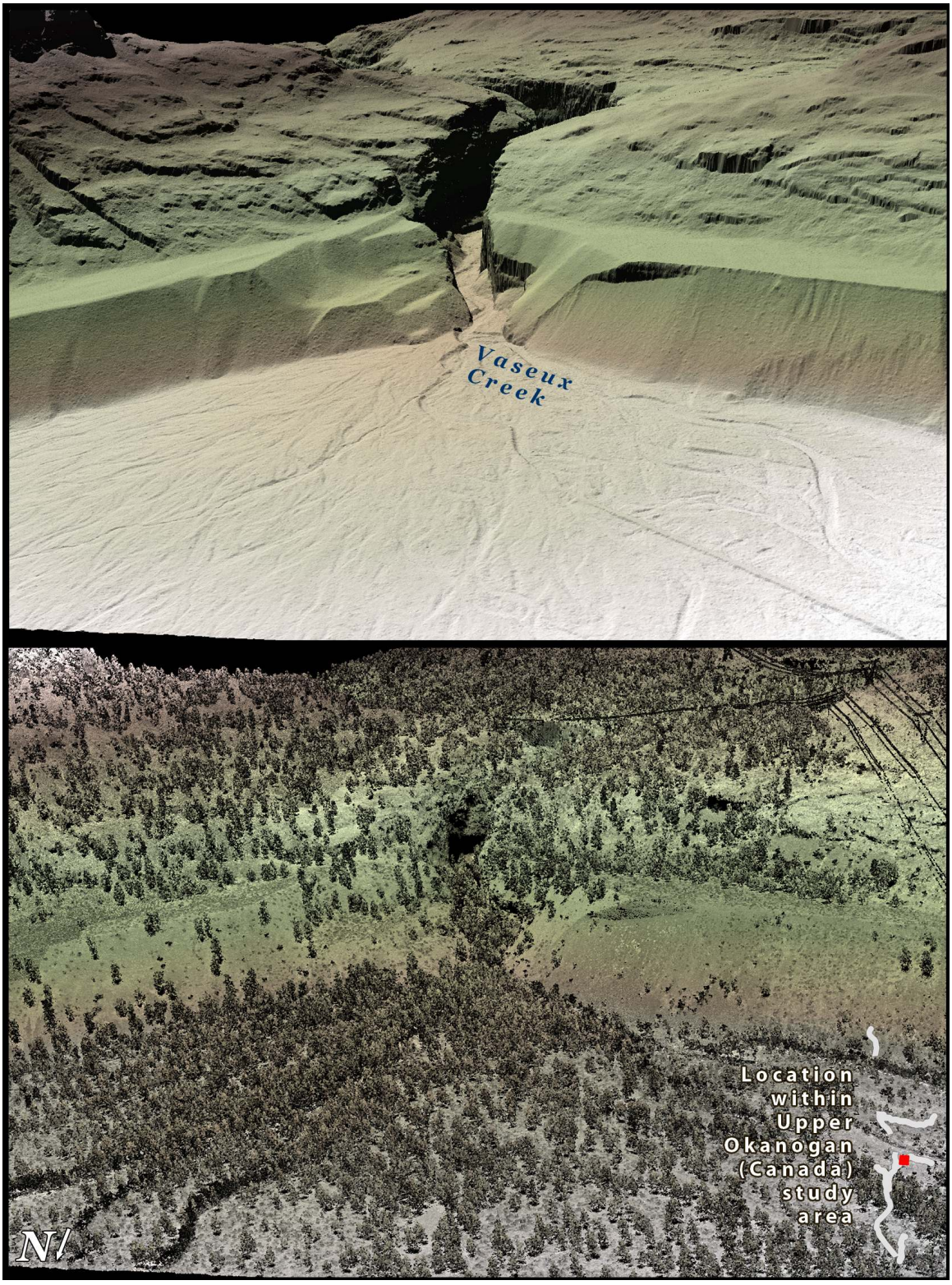

Figure 49. 3-d oblique view of LiDAR-derived surfaces in the western portion of quad 49119-B5 in the **Upper Okanogan, Canada, study area.** (Top image derived from ground-classified points, bottom image derived from all points).

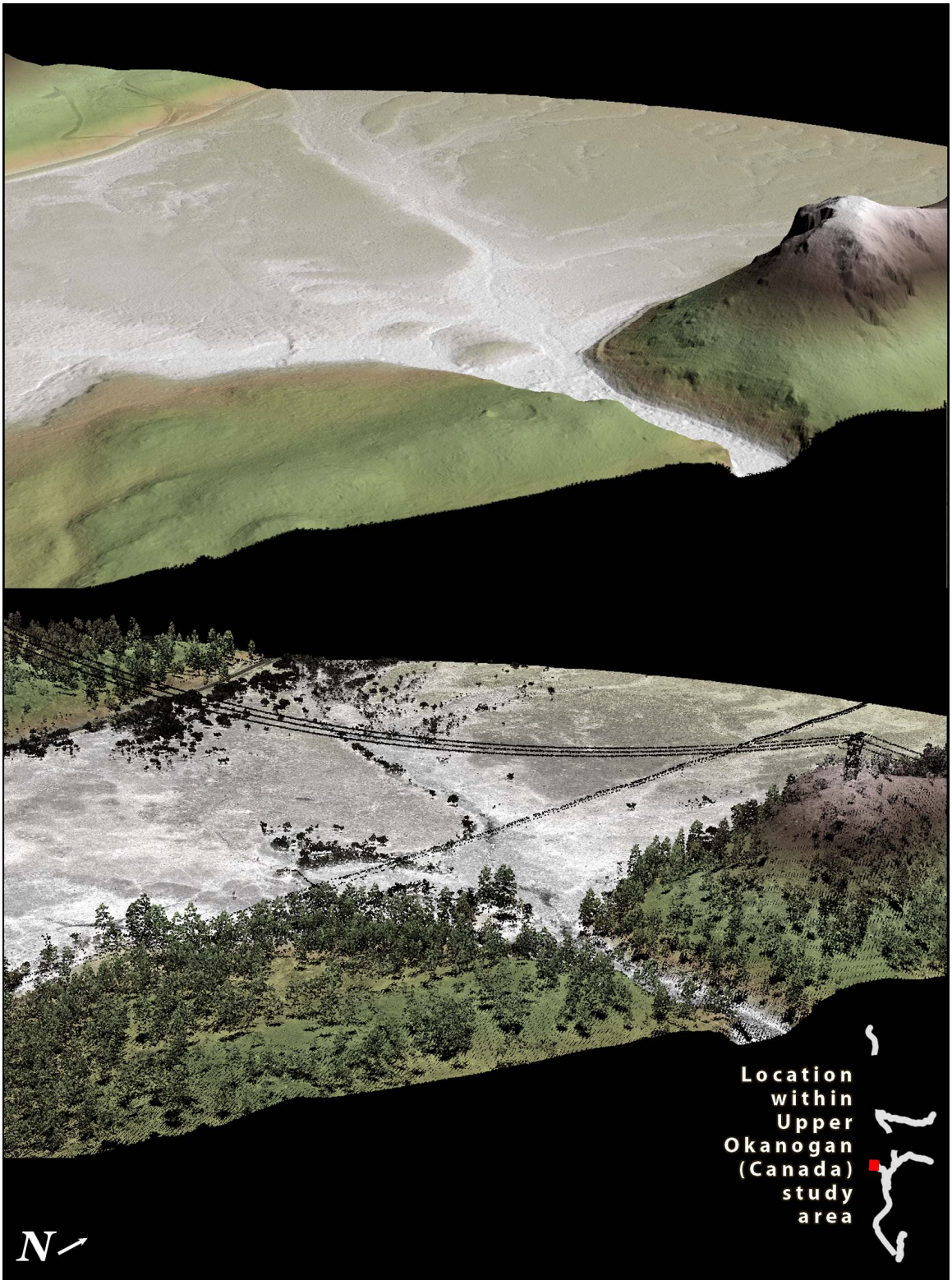

Figure 50. 3-d oblique view of LiDAR-derived surfaces in quad 49119-B5 along the Okanogan River in the **Upper Okanogan, Canada, study area.** (Top image derived from ground-classified points, bottom image derived from all points).

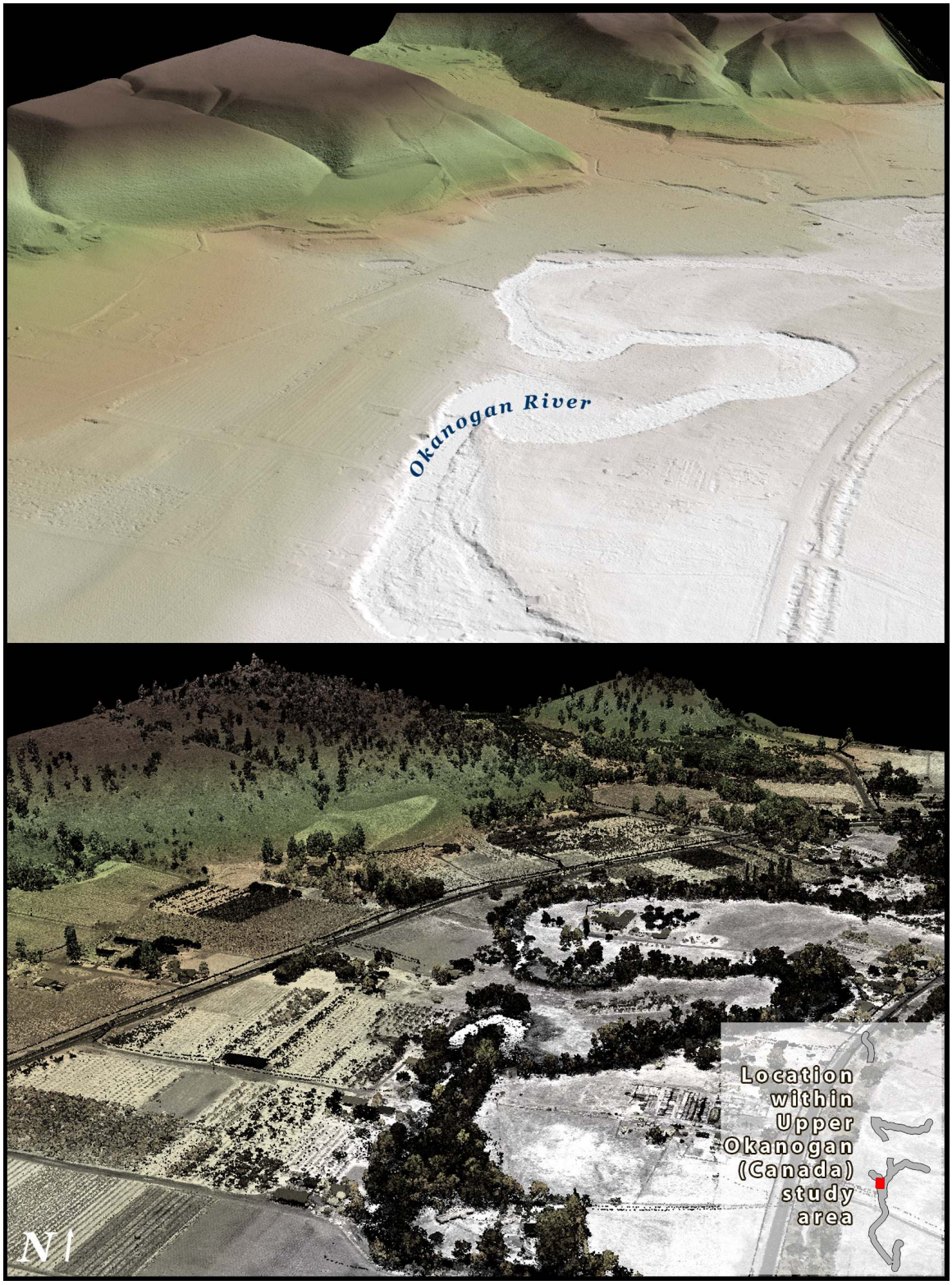

Figure 51. 3-d oblique view of LiDAR-derived surfaces in quad 48119-C5 at the mouth of Salmon Creek, in the southern portion of the **Lower Okanogan, Washington study area**. (Top image derived from ground-classified points, bottom image derived from all points).

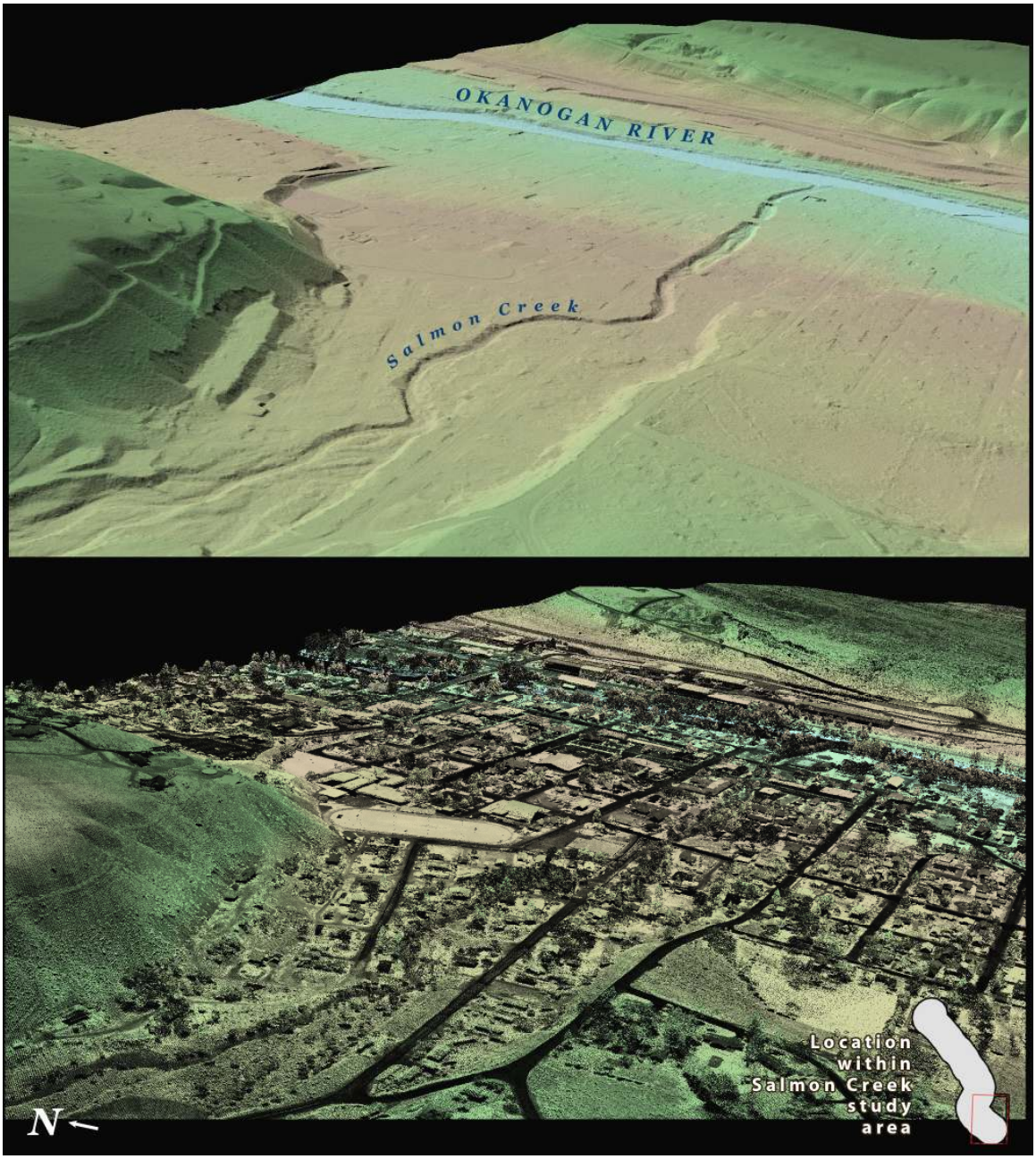

Figure 52. 3-d oblique view of LiDAR-derived surfaces in the northern portion of quad 48119-H4 of the Similkameen and Okanogan Rivers in the **Lower Okanogan, Washington study area.** (Top image derived from ground-classified points, bottom image derived from all points).

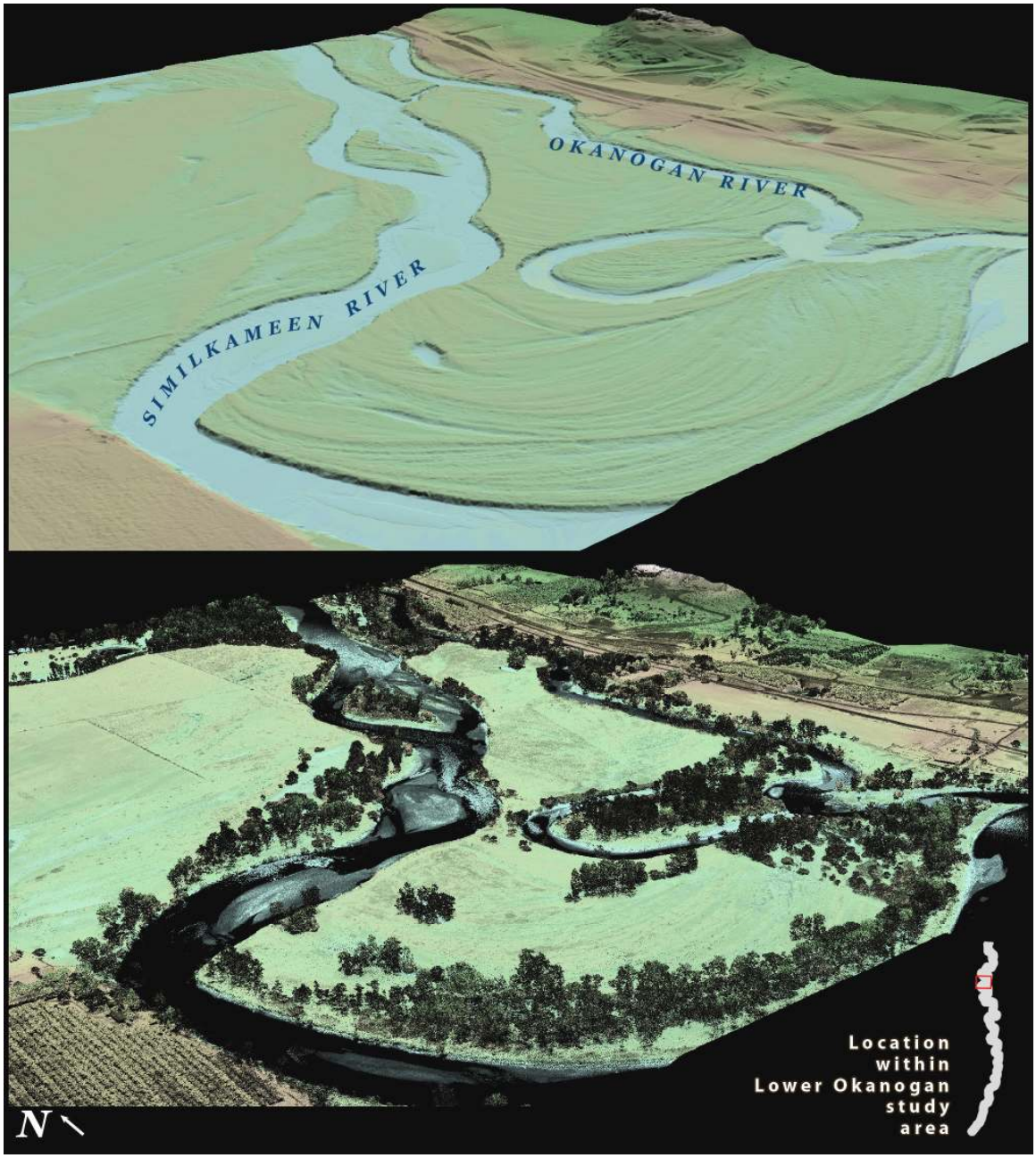

Figure 53. 3-d oblique view of LiDAR-derived surfaces in the southern portion of quad 48119-H4 of the Okanogan River in the **Lower Okanogan, Washington study area. (**Top image derived from ground-classified points, bottom image derived from all points).

Figure 54. 3-d oblique view of LiDAR-derived surfaces in quad 48119-G4 of the Okanogan River in the **Lower Okanogan study area.** (Top image derived from ground-classified points, bottom image derived from all points).

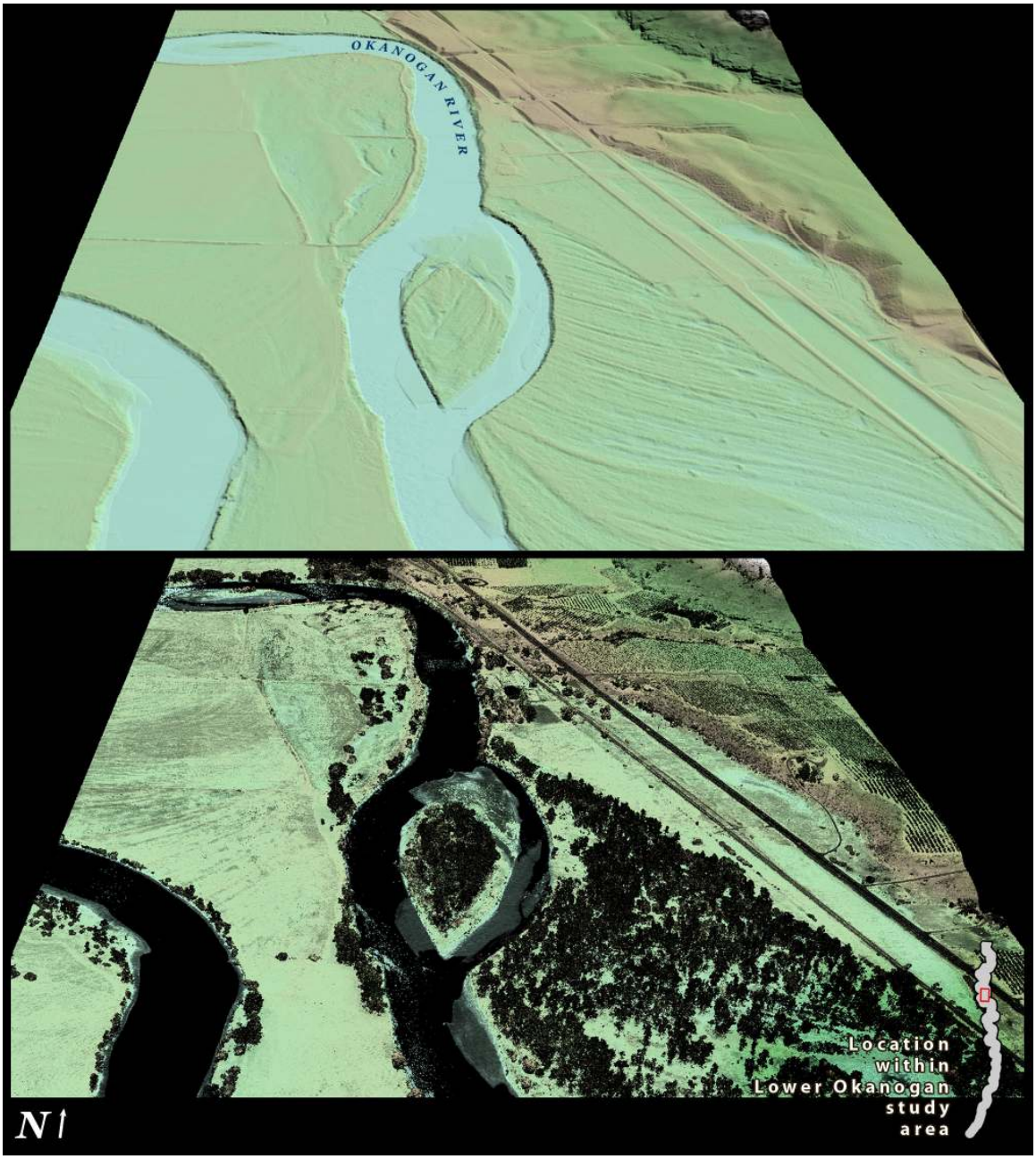

Figure 55. 3-d oblique view of LiDAR-derived surfaces in quad 44118-H8 along Desolation Creek in the **John Day, Oregon study area.** (Top image derived from ground-classified points, bottom image derived from all points).

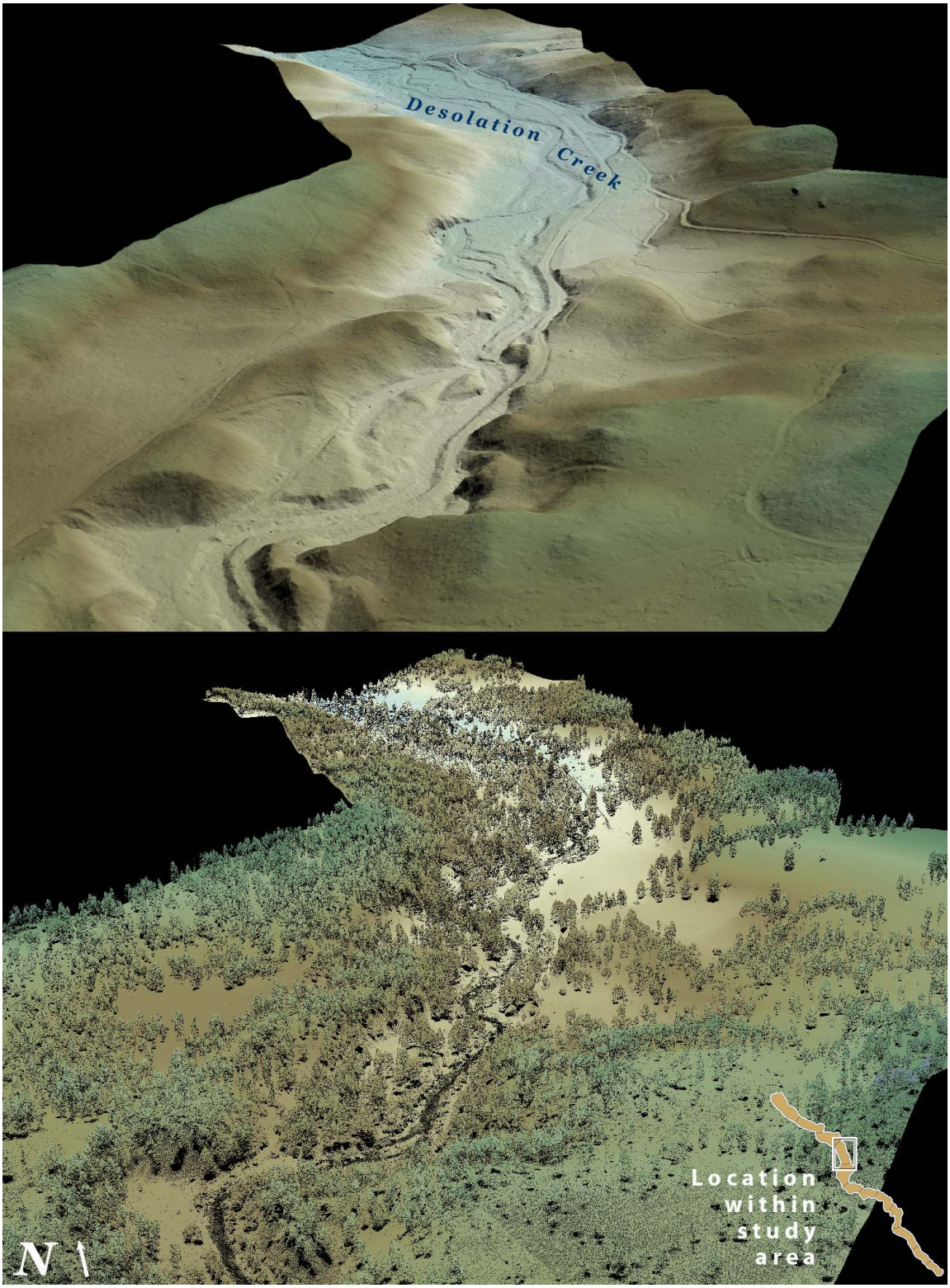

Figure 56. 3-d oblique view of LiDAR-derived surfaces in quad 44118-F7 showing the Middle Fork John Day River in the **John Day, Oregon study area.** (Top image derived from ground-classified points, bottom image derived from all points).

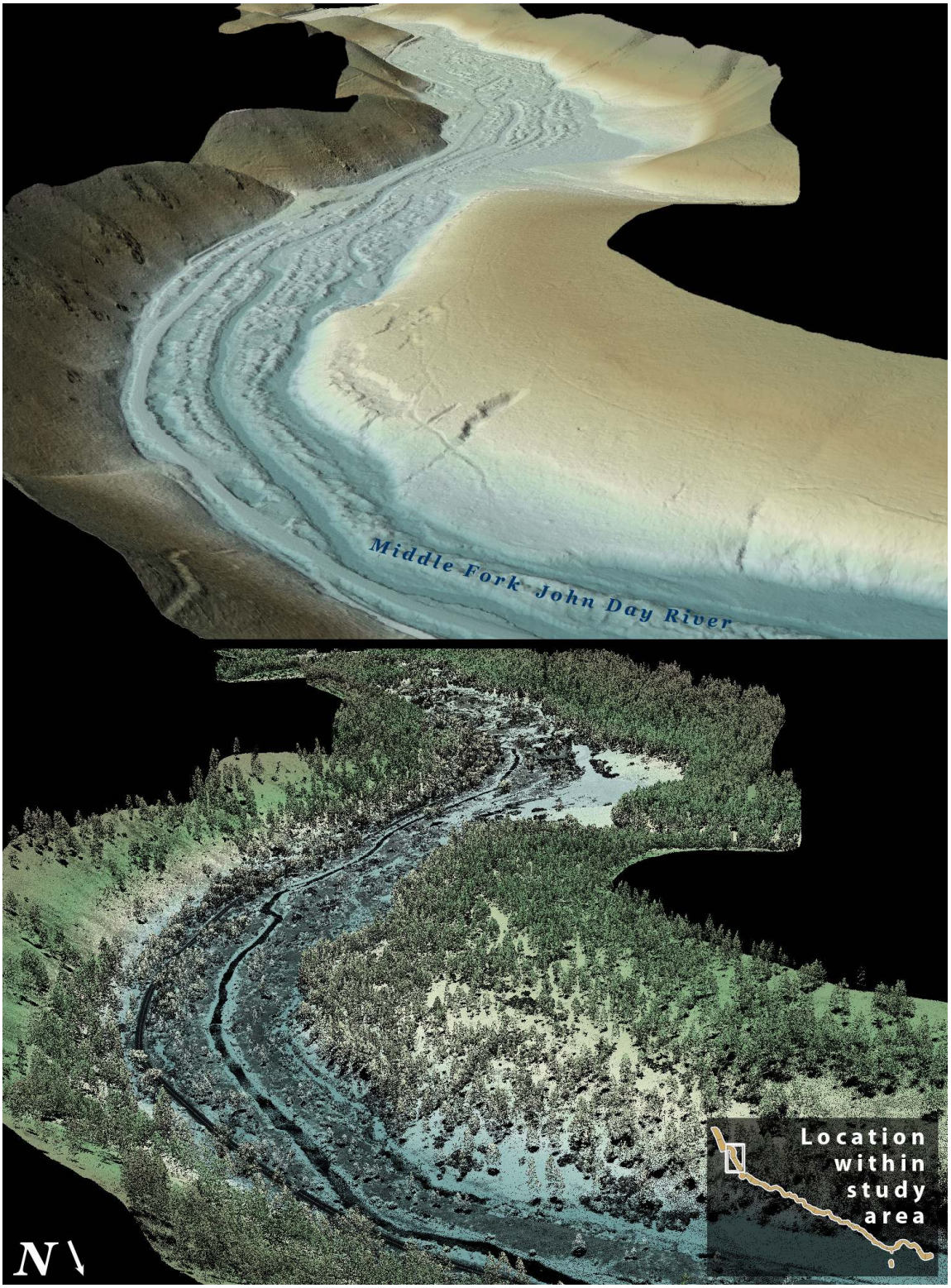

Figure 57. 3-d oblique view of LiDAR-derived surfaces in quad 44118-E5 showing the Middle Fork John Day River in the **John Day, Oregon study area.** (Top image derived from ground-classified points, bottom image derived from all points).

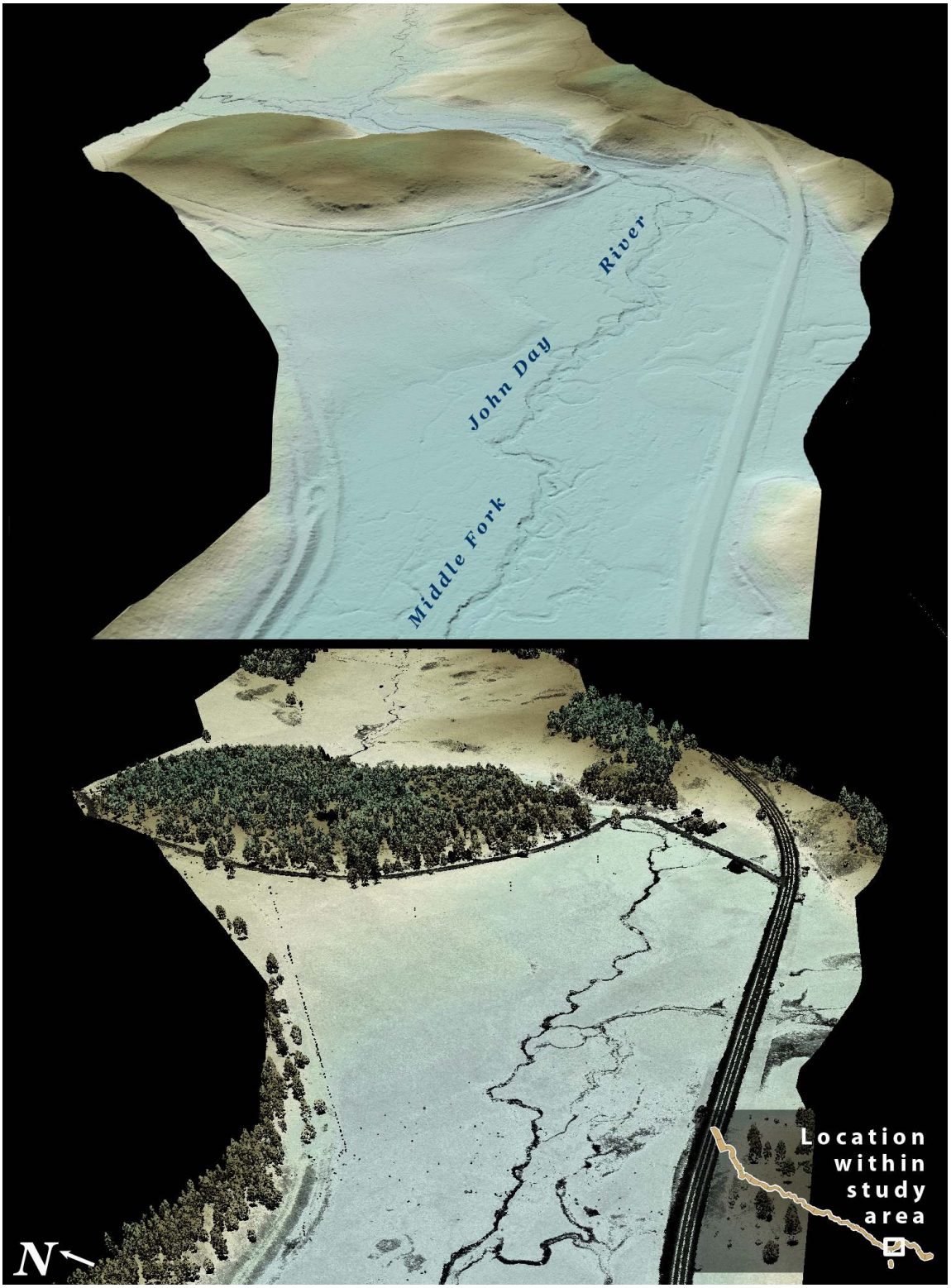

Figure 58. 3-d oblique view of LiDAR-derived surfaces in quad 48118-D6 along the John Day River in the **John Day, Oregon study area**. (Top image derived from ground-classified points, bottom image derived from all points).

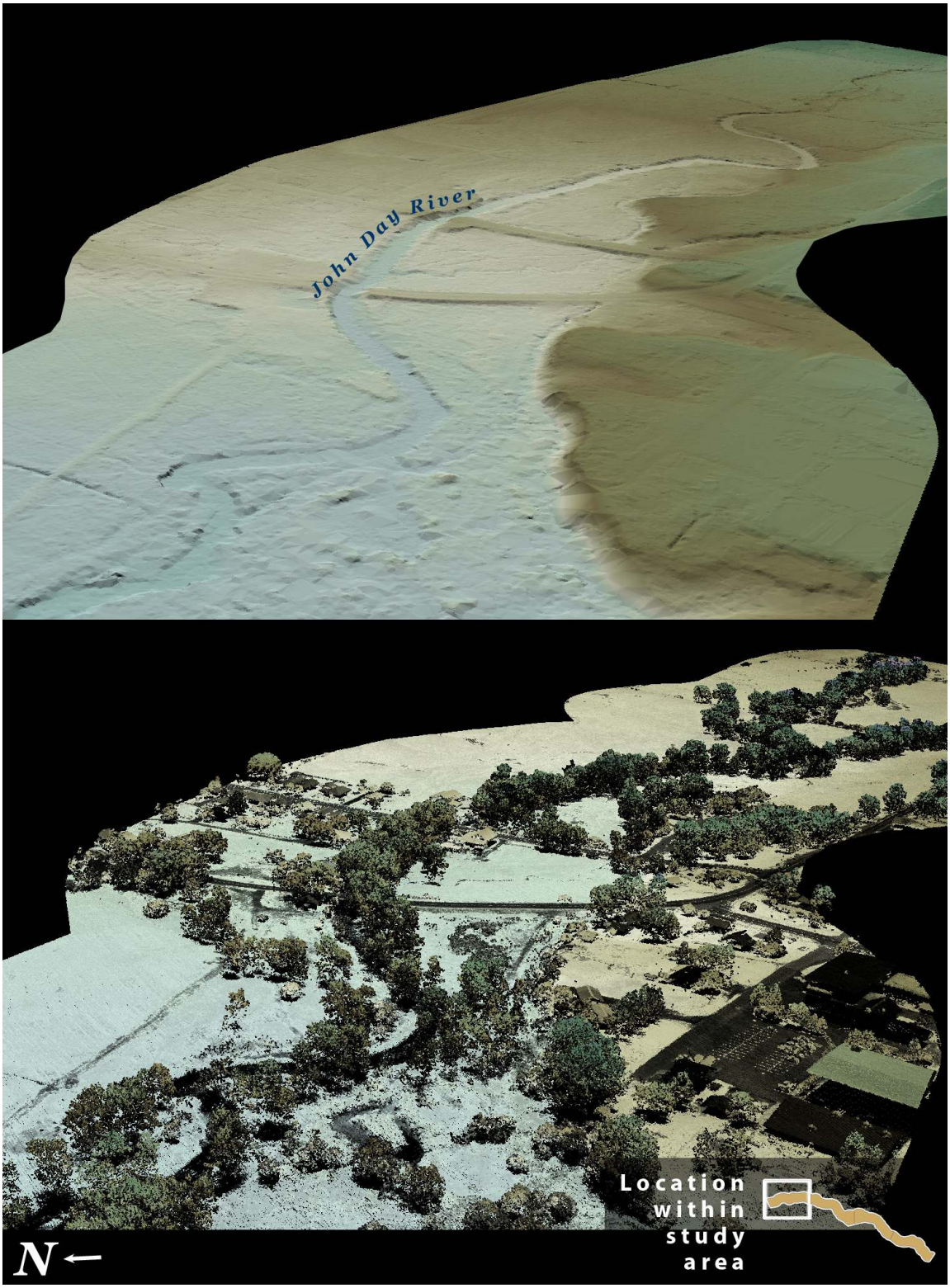

Figure 59. 3-d oblique view of LiDAR-derived surfaces in quad 47120-F3 / G3 along the Entiat River in the **Wenatchee, Washington study area**. (Top image derived from ground-classified points, bottom image derived from all points).

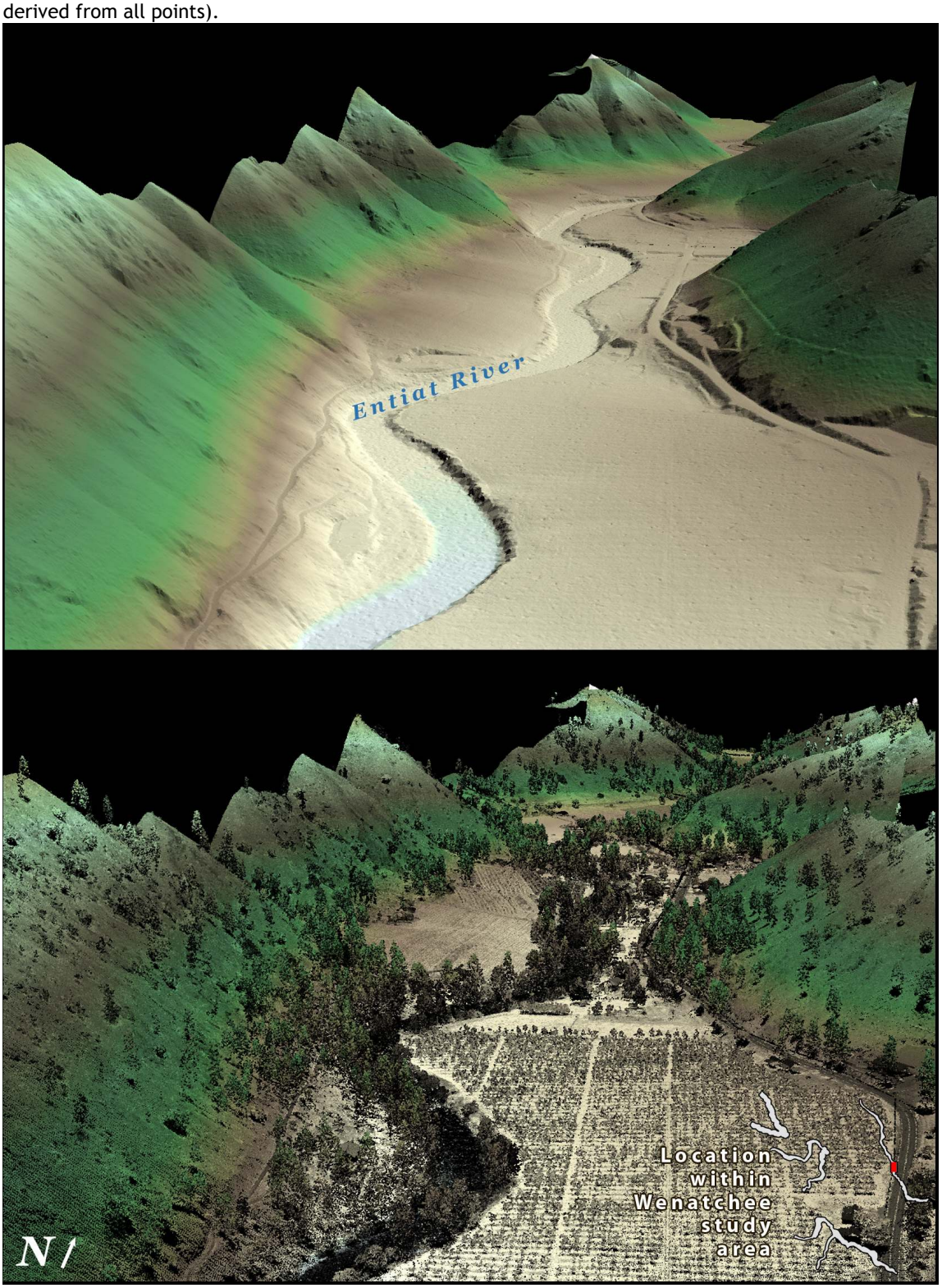

Figure 60. 3-d oblique view of LiDAR-derived surfaces in quad 47120-G6 along the Wenatchee River in the **Wenatchee, Washington study area**. (Top image derived from ground-classified points, bottom image derived from all points).

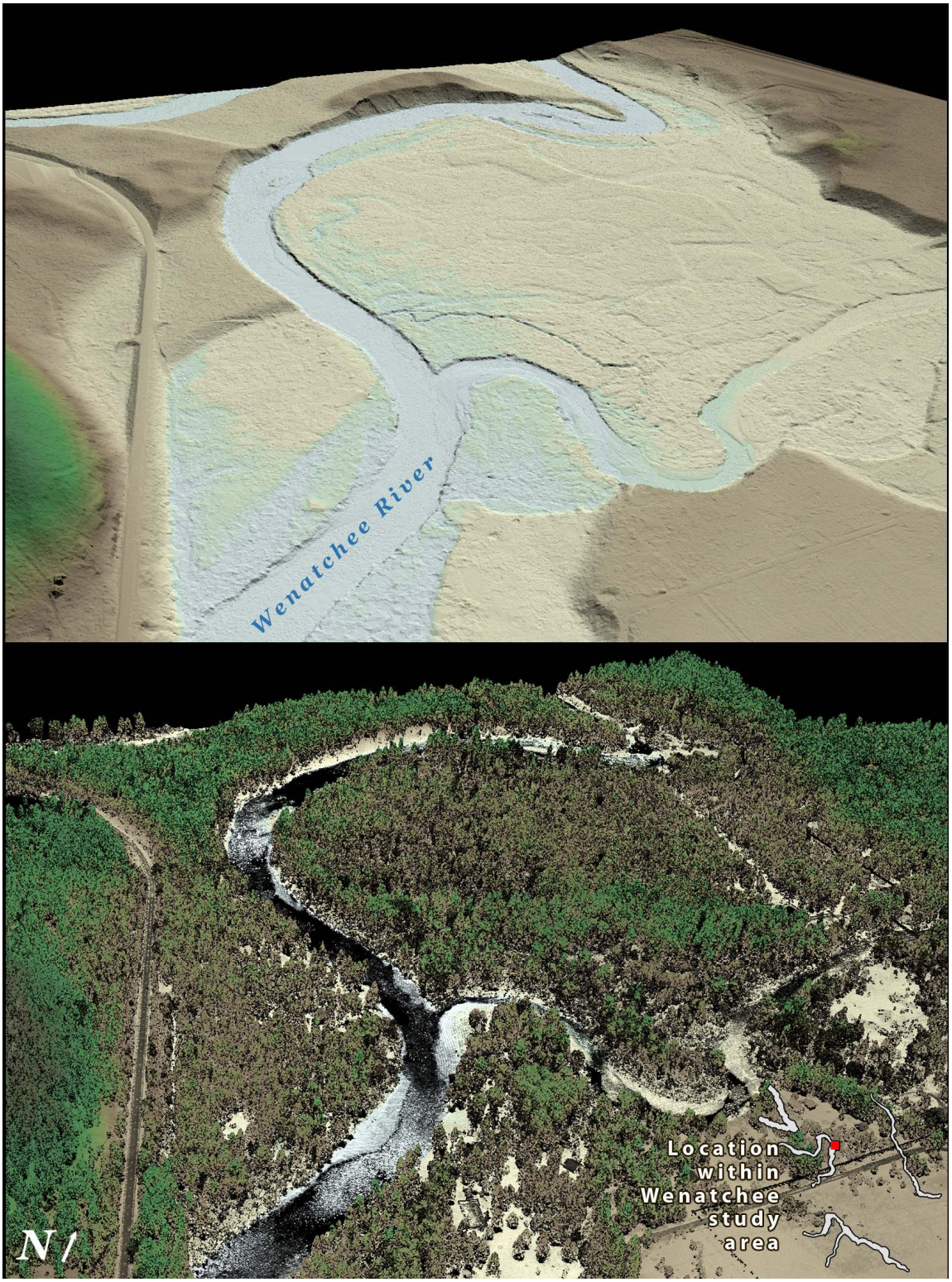

7. Glossary

1-sigma (σ) Absolute Deviation: Value for which the data are within one standard deviation (approximately 68th percentile) of a normally distributed data set.

2-sigma (σ) Absolute Deviation: Value for which the data are within two standard deviations (approximately 95th percentile) of a normally distributed data set.

Root Mean Square Error (RMSE): A statistic used to approximate the difference between real-world points and the LiDAR points. It is calculated by squaring all the values, then taking the average of the squares and taking the square root of the average.

Pulse Rate (PR): The rate at which laser pulses are emitted from the sensor; typically measured as thousands of pulses per second (kHz).

Pulse Returns: For every laser emitted, both the Leica ALS 50 Phase II and Optech 3100 LiDAR system can record *up to four* wave forms reflected back to the sensor. Portions of the wave form that return earliest are the highest element in multi-tiered surfaces such as vegetation. Portions of the wave form that return last are the lowest element in multi-tiered surfaces.

Accuracy: The statistical comparison between known (surveyed) points and laser points. Typically measured as the standard deviation (sigma, σ) and root mean square error (RMSE).

Intensity Values: The peak power ratio of the laser return to the emitted laser. It is a function of surface reflectivity.

Data Density: A common measure of LiDAR resolution, measured as points per square meter.

Spot Spacing: Also a measure of LiDAR resolution, measured as the average distance between laser points.

Nadir: A single point or locus of points on the surface of the earth directly below a sensor as it progresses along its flight line.

Scan Angle: The angle from nadir to the edge of the scan, measured in degrees. Laser point accuracy typically decreases as scan angles increase.

Overlap: The area shared between flight lines, typically measured in percents; 100% overlap is essential to ensure complete coverage and reduce laser shadows.

DTM / DEM: These often-interchanged terms refer to models made from laser points. The digital elevation model (DEM) refers to all surfaces, including bare ground and vegetation, while the digital terrain model (DTM) refers only to those points classified as ground.

Real-Time Kinematic (RTK) Survey: GPS surveying is conducted with a GPS base station deployed over a known monument with a radio connection to a GPS rover. Both the base station and rover receive differential GPS data and the baseline correction is solved between the two. This type of ground survey is accurate to 1.5 cm or less.

8. Citations

Soininen, A. 2004. TerraScan User's Guide. Terrasolid.